Integrated Master in Chemical Engineering

Iso-moisture: a new concept to predict moisture content in rayon cords and its influence on tire performance

A Master´s dissertation of

Lívia Coutinho Silva

Developed within the course of dissertation

held in

Continental Reifen Deutschland GmbH /Bound Compound & Reinforcement Technology Department

Supervisor at FEUP: **Prof. Fernão Magalhães**

Supervisor at Continental: **Dr. Thomas Kramer**

Departamento de Engenharia Química

February of 2020

Confidential Document. Use only for evaluation purposes.

This master thesis contains confidential information from Continental Reifen Deutschland GmbH. Duplication or distribution of the work, as well as the utilization or communication of its contents, is strictly prohibited without the express written authorization of Continental Reifen Deutschland GmbH, Jädekamp 30, 30419 Hanover.

Acknowledgment

First and foremost, I would like to thank God for his never-ending grace in my life, mercy and provision during all my life, and especially during my studies overseas.

Immeasurable appreciation and deepest gratitude for the help and support are extended to the following persons who in one way or another have contributed in making this study possible.

Fernando Silva, Joseli Coutinho and Bruna Coutinho Silva, my beloved parents and sister**,** for being a great family for me, for teaching me the ethical values and for always believing and supporting my dreams and my education.

Dr. Thomas Kramer, expert of Reinforcements at Continental and supervisor of this dissertation, for the opportunity to write this dissertation at Continental Tires headquarters facility and for the continuous scientific support throughout the project.

Prof. Fernão Magalhães, professor at FEUP and supervisor of this dissertation, for the scientific and technical support before and during the project.

Dr. Anuwat Suwannachit, senior development engineer at Continental, for being a great project leader, for all the patience, for the immense support with programming, for challenging me and inciting my creativity.

Eng. Christian Neufeld, Eng. Tiago Moura and Eng. Daniel Pinho, engineers at Continental, for all the support and for practical help on a daily basis.

Eng. Thomas Felten and Andreas Maibohn, colleagues from the testing laboratories at Continental, for all patience while teaching me to use the testing machines and for always giving me the information needed.

Débora Luiz and Paulo Marrocos, for being my best friends during my studies in Portugal, for making me feel more at home there and for always helping me even with the physical distance.

Jesse Rejek, for always motivating me to move to Germany, for helping with translations and for the great friendship.

Bruna Wanke and Isabela Campos, for always listening to my endless phone calls, for all the supporting during my doubts and for the great friendship.

Institutional Acknowledgment

Prof. Fernão Magalhães, supervisor of this dissertation, is an integrated member of LEPABE – Laboratório de Engenharia de Processos, Ambiente Biotecnologia e Energia, financed by: Base Financing - UIDB / 00511/2020 of the Research Unit - Laboratório de Engenharia de Processos, Ambiente, Biotecnologia e Energia – LEPABE - financed by national funds through FCT / MCTES (PIDDAC).

Abstract

There are different parameters involved in tire performance, such as rolling resistance, which are specified during the product design and are established according to the properties of the tire materials. The rolling resistance can be defined as the mechanical energy loss of the tire as heat, during the service for a given distance. Moreover, the vehicle's fuel consumption is tire-related which means that the lower the rolling resistance, the lower the fuel consumption.

In order to improve tire fuel efficiency by reducing rolling resistance, a reliable dynamic mechanical analysis (DMA) using rayon cords at different temperatures was conducted in this study. Rayon cords were chosen since they are used as textile reinforcements in tires and the results provide substantial information about the contribution of this material on the tire's overall rolling resistance. The characterization was challenging because rayon is a hygroscopic material, therefore, uptakes water vapor from the surrounding air. Factors that drive this phenomenon and the impact of the moisture content on the thermo-mechanical properties of the material have been investigated as well.

This study was divided into four main investigations, which were carried out before the first DMA trial. The first experiment aimed to analyze the diffusion of the water through the cured and uncured rubber used in tires and if it could reach the covered rayon cords. In the second test, the recovery of the tensile-strength of rayon cords after successive cycles of adsorption and desorption of water vapor molecules was investigated. Hysteresis elongation tests of rayon 1840x2 were carried out in order to perform the both studies described above. The third one consisted in using thermogravimetric analysis (TGA) to measure mass uptake of rayon 1840x2 at different atmospheric conditions of temperature (T) and relative humidity (RH), aiming to obtain data to plot sorption isotherms. In the fourth and last investigation, static tests at controlled atmosphere were performed to validate the data analysis from TGA for rayon 1840x2 and rayon 2440x2. Following that, the first DMA trial was finally performed.

In conclusion, as a consequence of the results obtained in this study, a new concept – **"iso-moisture"** – was created, experimentally validated and then approved by the Reinforcement R&D department at Continental Tires. This achievement enables one to choose appropriate atmospheric conditions (RH and T) to lead to a constant moisture content of rayon cords during the dynamic analysis, excluding then the effect of this variable in the results. As a following step, these results are used as an input to a finite-element simulation to predict the rolling resistance of tires, which helps to improve the design of the future tire.

Keywords: iso-moisture, rayon cords, dynamic mechanical analysis, moisture content control

Resumo

O desempenho do pneu envolve diferentes parâmetros, tais como, por exemplo, a resistência ao rolamento. Esses parâmetros são especificados durante o projeto do produto e estabelecidos a partir das properiedades dos materiais que constituem o pneu. A resistência ao rolamento pode ser definida como a perda de energia mecânica do pneu como calor, devido ao rolamento, numa determinada distância. Além disso, o consumo de combustível do pneu está relacionado com as propriedades dos materiais constituintes, dessa forma, quanto menor a resistência ao rolamento, menor o consumo de combustível.

Com o objetivo de melhorar a eficiência dos pneus através da redução da resistência ao rolamento, foi desenvoldo uma metologia de teste de análise dinâmico-mecânica (DMA), na qual cordões de rayon 1840x2 foram testados a diferentes temperaturas. Os cordões de rayon são utilizados como reforços têxteis no fabrico do pneu, assim, os resultados fornecem informações relevantes sobre a contribuição deste material na resistência ao rolamento global do pneu. A caracterização foi desafiadora uma vez que o rayon é um material higroscópico, ou seja, capta o vapor de água presente do ar. Os fatores que levam a este fenómeno e o impacto da humidade nas propriedades termo-mecânicas deste material também foram estudados.

Esta dissertação dividiu-se em quatro principais estudos. O primeiro tinha como objetivo analisar a possível difusão da água atráves da borracha curada e não curada de cordões de rayon calendrados. O segundo teste consistiu em verificar se a resistencia à tração do rayon é recuperada após sucessivos ciclos de adsorção e dessorção das moléculas de vapor de água. No terceiro estudo, foram realizadas análises termográvimétricas (TGA) do rayon em diferentes condições atmosféricas de temperatura (T) e humidade relativa (RH), com o propósito de obtenção de dados de forma a traçar as suas isotérmicas de adsorção. Na quarta e última investigação, foram realizados testes estáticos do rayon 1840x2 e rayon 2440x2, em condições atmosféricas controladas, a fim de validar a análise de dados realizada no estudo anterior.

Em suma, como consequência dos estudos realizados nas investigações acima mencionadas, um novo conceito – ***"iso-moisture"*** – foi criado, validado experimentalmente e então, aprovado pelo *Reinforcement R&D Department* da Continental Pneus. Esta conquista permite escolher condições atmosféricas apropriadas (RH e T) que levam a um teor de humidade constante nos cordões de rayon durante a DMA, excluindo o efeito desta variável nos resultados. Em seguida, estes resultados serão utilizados como entrada numa simulação de elementos finitos de forma a prever a resistência ao rolamento dos pneus para posterior redução da mesma, o que permitirá o *design* de pneus mais sustentáveis no futuro.

Palavras-chave: iso-moisture, cordões de rayon, análise dinâmico-mecânica, controlo de humidade

Declaration

I hereby declare, under word of honor, that this work is original and that all non-original contributions were properly indicated and referenced to the author with source identification.

Livia Coutinho Silva

Hannover, February of 2020

Index

List of Figures

List of Tables

Notation and Glossary

MC	Moisture content	%
T	Temperature	˚C
RH	Relative humidity	%
ΔG	Gibbs free energy change	J
ΔH	Enthalpy change	J
ΔS	Entropy change	$J \cdot {}^{\circ}C^{-1}$
A	Gas adsorbed in a surface	$g_{gas} \cdot g_{solid}^{-1}$
p	Equilibrium gas pressure	Pa
p_w	Water pressure	Pa
p_{ws}	Water saturation pressure	Pa
T_c	Critical temperature	K
P_c	Critical pressure	hPa
AH	Absolute humidity	$g \cdot cm^{-3}$
l	Original length of the cord	mm
Δl	Length of the cord change	mm
$\tan \delta$	Damping coefficient	
E'	Elastic modulus	$N \cdot mm^{-2}$
E''	Viscous modulus	$N \cdot mm^{-2}$
t	Time	h
ε	Strain	%
σ	Stress	$N \cdot mm^{-2}$
δ	Phase shift	˚

List of Acronyms

R&D	Research and Development
FTC	Federal Trade Commission
IUPAC	International Union of Pure and Applied Chemistry
TGA	Thermal Gravimetric Analysis
DMA	Dynamic Mechanical Analysis
-OH	Hydroxyl Group
3D	Three Dimensional
MHG	Modular Humidity Generator
MPT	Multi Purpose Testware
MPE	Multi Purpose Elite
FFT	Fast Fourier Transform

1 Introduction

1.1 Framing and presentation of the work

This master dissertation is part of a long-term project called *Cord Material Model* within the Continental Tires Division in Hannover, Germany. This project aims to simulate the mechanical behavior of the different material cords present in a tire. For that, each cord must be characterized experimentally in order to obtain specific parameters which will be used as an input to a finite-model simulation to predict tire performance.

Tire performance involves different parameters, such as rolling resistance, which are specified during the product design. The rolling resistance can be defined as the mechanical energy loss of the tire as heat, because of tire rolling for a given distance[1]. The consumption of energy by the tires is related to the fuel consumption of the vehicle, therefore, the design of a tire with lower rolling resistance leads to a lower fuel consumption as well. The rolling resistance and the other parameters are given by the properties of the tire's constituent materials, which can be obtained by characterization techniques.

This master thesis focuses on the characterization of rayon cords, which are textiles used as tire reinforcements. A lot of knowledge was previously developed for other textiles and it was used as an important background for this present work. Therefore, for a deeper understanding of the present topic, it is recommended the reading of the two previous master theses written at Continental regarding characterization of textile cords: "Hysteresis in Tire Textile Reinforcements focusing on PET material" from André Cardoso and "Hysteresis in Tire Textile Reinforcements" from Mariana Gomes.

The real challenge of this master thesis was to develop a test method to obtain the dynamic response of rayon cords under different conditions (temperature, frequency and amplitude) without the influence of moisture content. That is because rayon is a hygroscopic material and uptakes the water from the surrounding air until it reaches the equilibrium. The change of moisture content of the rayon cords alters the mechanical response of it, therefore, the moisture content must be constant in order to achieve reliable results during the characterization of the material.

There is not much information available on literature about rayon material, how it interacts with water vapor and how the moisture content affects the mechanical response. So, new tests methods were firstly developed besides the DMA technique in order to answer some fundamental questions and to guarantee a further reliable characterization of the rayon cords.

1.2 Continental Group

Continental AG is a multinational company founded in 1871 in Germany. It is present in more than 50 countries, operating more than 400 facilities. Continental is divided into 5 divisions focusing on different products: Chassis & Safety; Interior; Vitesco Technologies; Tires and Conti Tech.[2]

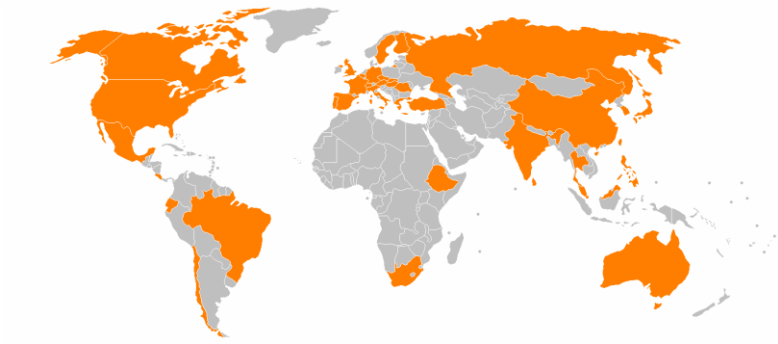

Figure 1: Continental AG global locations.[2]

Continental Tires: that is the oldest division of the group. It manufactures tires for different vehicles, such as passenger cars, commercial vehicles and two-wheelers.[2]

Continental Chassis & Safety: develops products to support vehicle dynamics and produces integrated active and passive driving safety technologies. The product portfolio ranges from electronic and hydraulic brake and chassis control systems to sensors.[2]

Continental Interior: develops systems integrating hardware and software components that dynamically adapt to the user's preferences, needs, and situation and environment. A few examples of the portfolio are: multimedia systems, connection of mobile devices, climate control, control panel, intelligent street lighting, glass control and antenna modules and comfort locking systems.[2]

Vitesco Technology: develops innovative, efficient electrification technologies for all types of vehicle. Its portfolio includes 48-volt electrification solutions, electric drives, and power electronics for hybrid and battery-electric vehicles. Furthermore, the product range counts electronic controls, sensors and actuators as well as solutions for exhaust after-treatment.[2]

Continental Conti Tech: offers products and systems made of rubber and plastic in combination with metal or fabric. In cooperation with electronic components, new solutions are created for different purposes, such as: fluid handling, drive systems, blends, printing technologies, sealing systems, suspension and vibration damping and surfaces.[2]

This project was developed in the R&D (Research and Development) facilities of Continental headquarters in Hannover (Germany), at Continental Tire division.

1.3 Contribution of the author to the work

Rayon is a hygroscopic material and quickly (order of minutes) adsorbs the water vapor from the surrounding air, modifying its mechanical properties. There is not much in the literature about rayon structure and its interaction with water vapor because it is a challenging material to be experimentally tested, due to the reason mentioned above.

This thesis distinguishes from the others for the following reasons: it is the first deep study done about the rayon material at Continental, it answers some previous open questions regarding the unexpected behavior of rayon cords under dynamic conditions and proves the importance of moisture control. Therefore, the accomplishment of this master dissertation allows new possibilities to the future expansion of knowledge regarding textile reinforcements used in tires.

First, it is important to notice all the achievements accomplished with this master thesis:

1. Test method development to characterize rayon cords under dynamic conditions
2. Creation of an original test method for “iso-moisture” tool drawing up.
3. Drawing of sorption isotherms for rayon cords at 20 ˚C, 30 ˚C, 40 ˚C, 50 ˚C and 60 ˚C.
4. Build up diagram where it is possible to read the moisture content within rayon for different ambient conditions (temperature and relative humidity)
5. Proof that the water vapor diffuses through the rubber used in tires (new test method was developed for that)
6. Proof the tensile strength upper-limit of rayon cords depends on the moisture content, that is higher for atmospheres at elevated T and RH.
7. Proof the mechanical properties of rayon cords are recovered after successive cycles of sorption and desorption of moisture (new test method was developed for that)

The learnings from this present master thesis has an essential contribution to different departments at Continental Tires Division, such as Test Method Development, Material Simulation, Material Process Development and Industrialization, Product and Supply Quality Control and Manufacturing.

1.4 Organization of the thesis

This Master Thesis is organized into 6 chapters. The main purpose of each chapter is briefly described as follows:

Chapter 1 – Introduction: this section introduces the framework of the thesis to the reader; presents the company Continental AG; the motivation for this project and its main contributions.

Chapter 2 – State of Art: explains the topic in more details. It starts with a general overview about tires, including its main components and materials. It is followed by the two principal theories in which this master thesis was based on. One is the adsorption phenomena between a solid and a gas and its equilibrium theory. Another is the thermodynamics of the air moisture, including how temperature and relative humidity are related to each other. Finally, insights about the characterization parameters obtained from the dynamic mechanical analysis are presented.

Chapter 3 – Material and Methods: describes the methodology adopted for each test carried out, mentioning the machines, sample conditioning and materials used. This section is composed of four sections and it allows the future repetition of the work done. Some of the tests described are: thermal gravimetric analysis (TGA), hysteresis elongation and dynamic mechanical analysis (DMA).

Chapter 4 – Results and Discussion: presents accurate description of the data evaluation a self-critical analysis of the work done. It is divided in four section and each one follows one of the test methods described in Chapter 3.

Chapter 5 – Conclusions: resumes the main goals achieved during the project and its main contributions to Continental.

Chapter 6 – Assessment of the Work Done: the degree of accomplishments of the objectives are described, the limitations perceived throughout the thesis and suggestions for the future work.

2 Context and State of the art

2.1 Tire technology

Tires are highly engineered products designed to meet specific criteria of quality, performance and safety. The primary function of a tire is to provide the interface between the vehicle and the highway. The highway surface can be wet, dry, snow-covered or ice-covered, those conditions led to complex effects on the tire tread. Besides that, the tires support the vehicle load and are responsible for the road surface friction. The latter allows a vehicle to start, stop and turn corners. Finally, tires act as a spring and damper system to absorb impacts and the road surface irregularities under a wide variety of operating conditions.[3] A scheme with the main components of a passenger car tire is showed in Figure 2.

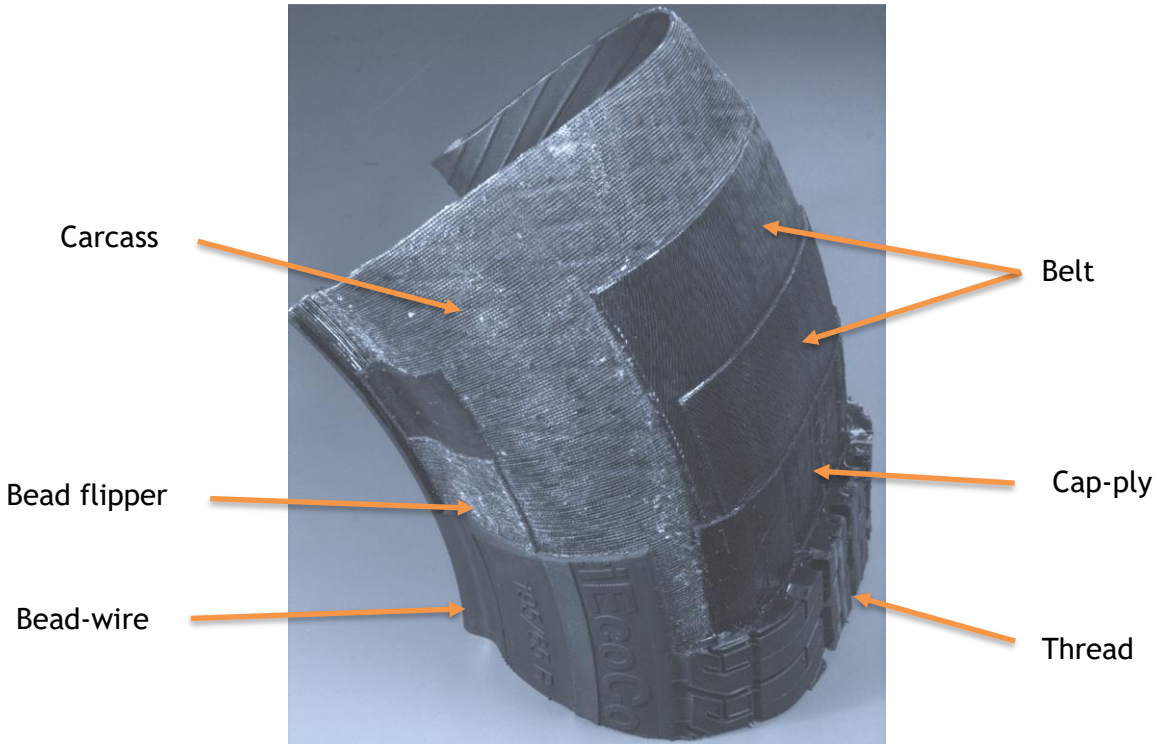

Figure 2: Main components of tire passenger car. Adapted from reference 4.

2.1.1 Tire materials

Tires are not only made of rubber; but also consist of different materials in which the weight percentage varies from tire to tire according to the ultimate application and the tire performance expectation of the customer.

Continental produces tires for different vehicle types, including passenger car, trucks, buses, vans, etc. For each of them, there is a specific design which leads to a material distribution within the tire. There is also a variation of the design within the same category for different vehicles models and brands, but that is not as highly noticed as when two types are compared.

The typical weight proportion of the ingredient used to manufacture a passenger car and truck tires is described in Figure 3.

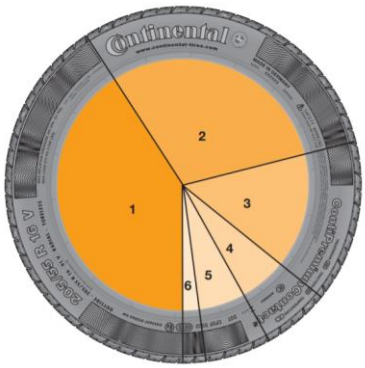

Figure 3: Breakdown of tire ingredients. Adapted from references 4 and 5.

1 32 % - **Rubber:** natural and synthetic

2 30 % - **Active Fillers:** carbon black, silica, carbon, chalk

3 24 % - **Reinforcing materials:** steel, polyester, rayon, nylon

4 6 % - **Plasticizers:** oils and resins

5 6 % - **Chemicals for vulcanization:** sulphur, zinc oxide, other chemicals

6 2 % - **Anti-ageing agents and other chemicals**

2.1.2 Tire reinforcements

Each material presented in section 2.1.1 has an impact on tire manufacturing and performance. Rubber (synthetic + natural) is the main component of the tire, followed by reinforcing materials, see Figure 3. Those reinforcing materials are textiles or metals cords and are the predominant load carrying of the cord-rubber composite.[3]

Each reinforcement has specific thermo-mechanical properties that will influence the tire's overall performance, and they are placed in different tire components during the design. For example, rayon and polyester cords are placed in the carcass to control internal pressure and maintain the tire's shape. Nylon and aramid are in the bead flipper to enhance directional stability and to give steering precision.[5]

The tire reinforcement is related to the rolling resistance as well as the rubber. The rolling resistance is one of the parameters regarding tire performance, and it is defined as the mechanical energy loss of the tire as heat, because of tire rolling for a given distance (see more details in section 2.4).[1] Thus, understanding how the reinforcements affect tire performance has great importance for the design of future tires, which are desired to have a reduced rolling resistance, which will lead to lower vehicle fuel.[5]

For this present work, there is a focus on one the textile reinforcements material named viscose rayon.

2.2 Viscose rayon: a tire textile reinforcement

Rayon is a regenerated cellulose fiber, that is, a type of manufactured or man-made fiber which requires cellulose (mainly from wood or plant fibers) as raw material.[6] Those fibers were the first human-made fibers applied in the textile industry and were commonly known as “artificial silk” during the 1850s. Nowadays, it is frequently found in literature the term “synthetic silk”.[6]

The different regenerated cellulose fibers are classified according to their production method. There are four main types of rayon fibers: viscose, lyocell, cupro and acetate.[6,7] This work focuses on the viscose rayon, which is the type of rayon used as a tire reinforcement.

2.2.1 Chemistry of viscose rayon formation

The viscose process was first patented by Cross and Bevan in England in 1893. Over the 20th century, the viscose process has undergone many refinements, but the basic chemistry is still the same.[7] A schematic of the chemistry of the viscose rayon process is given in Figure 4.

The raw cellulose from wood or cotton is steeped in and boiled with caustic soda forming soda cellulose. This step removes the non-cellulose content, such as the hemicellulose and the lignin. Carbon disulfide is added to react with the soda cellulose, forming sodium cellulose xanthate. Finally, the solution is neutralized with dilute sulfuric acid, and the cellulose structure is recovered.[6,21]

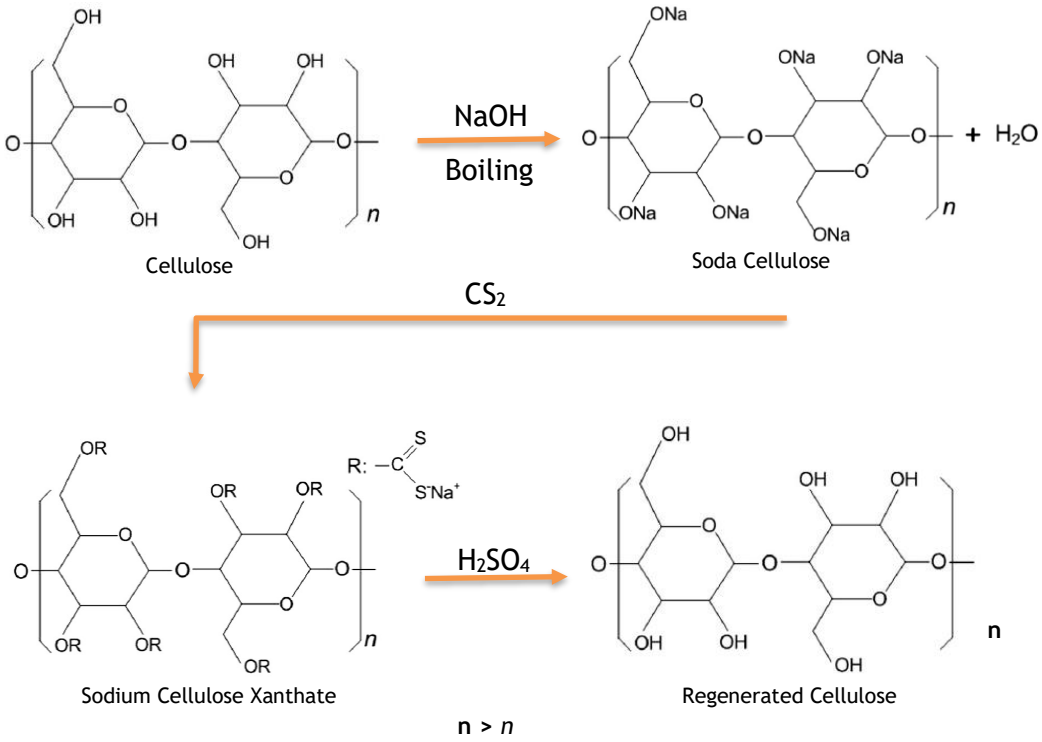

Figure 4: A scheme of the chemistry of viscose rayon production. Adapted from reference 6.

According to the U.S. Federal Trade Commission (FTC), rayon cannot have more than 15 percent of the hydrogen of the hydroxyl groups replaced by the substituents during its production process.[8] The remaining 85 percent of hydroxyl groups gives the hygroscopicity property of rayon.[6]

Rayon is generally resistant to heat up to about 150 °C but loses strength on prolongated exposure and more rapidly at higher temperatures. It starts to decompose at around 210 °C. Furthermore, rayon is susceptible to microbiological attack and has a smooth appearance.[21]

2.3 Water vapor molecules interaction with rayon cords

Rayon fiber and its hygroscopic chemist were introduced in Section 2.2. The drop in the stiffness of cellulose-based materials occurs due to the presence of moisture has been proved.[10] Thus, understanding what is behind the water uptake by rayon cords is crucial to improve its characterization methods.

One of this master thesis' objective is to understand the relation between the concentration of water vapor in the atmosphere and the concentration of water vapor in the rayon cords. The air moisture gives the amount of water in the atmosphere; therefore, it is essential to perceive how the water behaves in the air for different temperatures and how to describe it. This section brings some concepts regarding air moisture and how it interacts with rayon cords.

2.3.1 Moisture uptake behavior of Cellulose Fibers

Cellulose fibers are inherently hydrophilic owing to the presence of a high amount of hydroxyl groups (-OH) available within its chemical structure. Even though cellulose has a high OH to C ration, not all the hydroxyl groups are exposed or accessible, as cellulose is semi-crystalline. The highly crystalline region of cellulose is inaccessible to water molecules. On the other hand, the water molecules can penetrate and gain access into the amorphous region of cellulose.[10]

As the cellulose fibers adsorb the water molecules, they swell up due to the molecules occupying the space in between the microfibrils. The water molecules within the natural fibers can either form a monolayer, which associates closely with the available -OH groups, or form a multilayer at which not all water molecules are in intimate contact with accessible -OH groups.[10]

2.3.2 Adsorption of water vapor into rayon cords

When molecules of a substance, which are present in a gas phase, are brought in contact with a solid, a part of them spontaneously moves from the fluid into the solid. The displaced molecules either penetrate into the solid or remain on the outside, attached to its surface. The spontaneous accumulation of a gas or vapor at the solid surface as compared to the bulk surface is called adsorption.[11]

At adsorption phenomena, the solid that captures the gas is called adsorbent, while the gas which was taken up by the solid is called adsorbate.[11] A scheme of an adsorption process between water vapor molecules and rayon cords is showed in Figure 5.

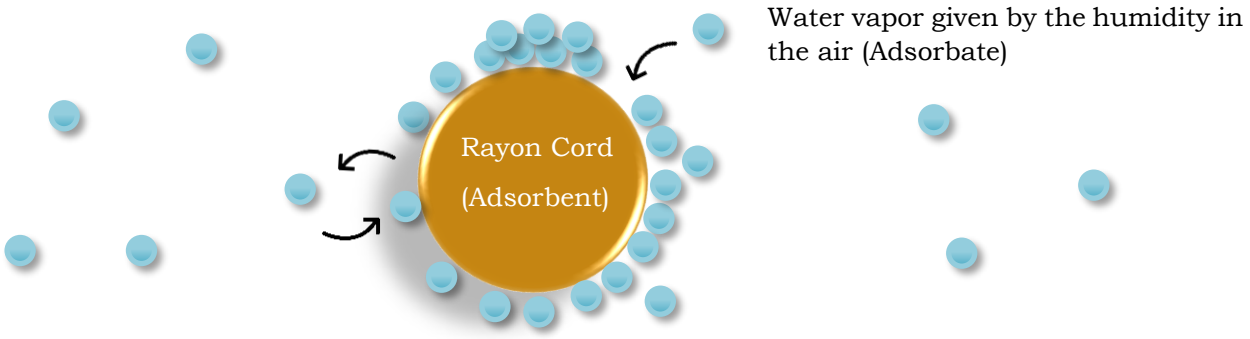

Figure 5: Water molecules adsorption in rayon cords process scheme.

When the gas comes to the solid surface, two different sorption mechanisms may happen. There is either a weak interaction between solid and gas, called physical adsorption, or strong interactions, named chemical adsorption. The first implies the same forces that are active in condensation and evaporation processes; that is, only physical bonds are formed between the molecules, e.g. Van der Waals interaction (London dispersion, dipole-dipole) and hydrogen bonding. Those week bonds can be broken, leading to a reversible phenomenon called desorption. For the latter one, ionic or covalent bonds are formed between the adsorbent and the adsorbate.[12,13] The chemical adsorption is not on the focus of this project; therefore, mentioning adsorption means physical adsorption.

The rayon cords used in tire manufacturing are firstly rubberized through a calendering process, in which a skim compound (type of rubber) is embedded in the textile fabric. Later, the calendered material follows the standard tire curing process. Consequently, at a tire production

line, the rayon cords are not freely exposed to the air as the scheme presented in Figure 5, but rather protected by the rubber matrix.

The solution-diffusion model is used to describe the gas molecules permeation in a rubber matrix. When rubber is exposed to a gas, a solution occurs at the surface, and the dissolved gas molecules diffuse into the interior. That happens due to the free volumes or “holes” available in between the molecular chains present in the rubber matrix. Those “holes” thermally form and disappear with the movement of polymer chains. The water molecules, therefore, migrate from “holes” to “holes” until they reach the rayon cords, when the adsorption starts.[14] A scheme of the solution-diffusion model of water molecules in rubber combined by the adsorption by rayon cords is illustrated in Figure 6.

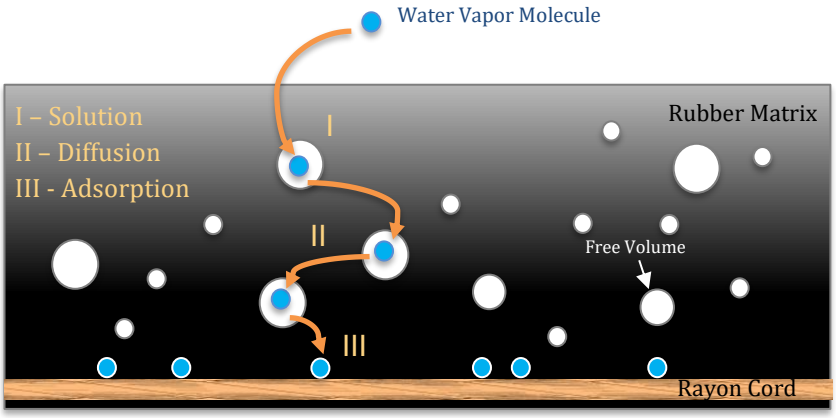

Figure 6: Scheme of water vapor molecules permeation into rubberized rayon. Adapted from reference 15.

2.3.3 Equilibrium of adsorption

As describes in section 2.3.2, adsorption is a spontaneous process of transferring material from a fluid phase to a solid phase. Mass transfer and thermodynamics are used to explain this separation process. The mass will be continuously transferred from the gas to the solid (adsorption) and from the solid to the gas (desorption) at different rates. The rate will finally equal when the equilibrium is reached, that is, when Gibbs free energy equals to zero. [13]

The adsorption is a spontaneous process; therefore, it requires a negative Gibbs free energy ($\Delta G < 0$). The Gibbs free energy is well-known from the following equation (1):[12]

$$\Delta G = \Delta H - T \cdot \Delta S \quad (1)$$

Where ΔH is the enthalpy and ΔS is the entropy.

Adsorption involves the adhesion of atoms to a surface, that is, restriction of motion. That means entropy decreases together with the reduction of the degrees of freedom of the adsorbed species. To compensate for this - and for the species to be able to adsorb to the surface - heat must be released as they adhere to each other. Hence, adsorption should be an exothermic process.[13]

The adsorption equilibrium depends on the temperature, gas vapor pressure and specific surface area of the solid. The nature of the solid or gas also plays a significant role in that phenomena as it will influence the formation of the physical bonds that were mentioned in section 2.3.2. The specific area gives available area of material for the exchange of molecules.[12,13]

For a particular substance, the adsorption equilibrium can be written as a general equation:

$$A = f(p, T) \tag{2}$$

Where A is the quantity of gas adsorbed on the surface per unit of mass or mol of adsorbent, p is the equilibrium pressure of the gas in the bulk phase, and T is the temperature. For high-pressure systems, that is, pressure above the saturation pressure, adsorption is not dependent on pressure.[12]

When studying adsorption equilibrium, one of the parameters remains unchanged. Depending on which variable is fixed, different relations for the left variables can be achieved. Those relations and the variables involved are summarized in Table 1.

Table 1: Different types of relations when studying adsorption phenomena.[12]

Name	*Fixed Variable*	*Relation*
Adsorption isotherm	Temperature	$A = f(p)_T$
Adsorption isobar	Pressure	$A = f(T)_p$
Adsorption isostere	Amount of gas adsorbed	$p = f(T)_a$

This study focuses on the adsorption isotherms; in other words, the relation between the amount of water vapor in the air and in the rayon cord, at a constant temperature. The isotherms can show different shapes which vary with the adsorption mechanisms: monomolecular adsorption, multimolecular adsorption and condensation in pores or capillaries. According to IUPAC (International Union of Pure and Applied Chemistry), the isotherms are classified into six characteristics types, and an example is showed in Figure 7.[15]

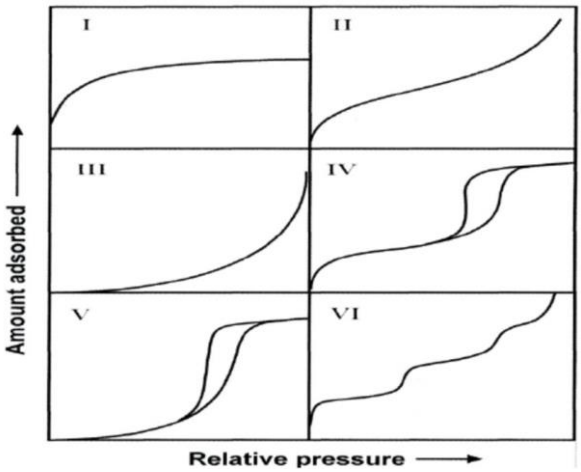

Figure 7: Different types of isotherms classified by IUPAC.[15]

In the x-axis of the isotherm, the amount of substance in the gas phase is represented as concentration, gas pressure or relative pressure. In the y-axis, the amount of substance on the solid phase, *A*, is represented in concentration or mass percentage (dry basis or wet basis).[15]

2.3.4 Sorption isotherms

Rayon continuously exchanges moisture with the ambient air due to its hygroscopicity. An equilibrium moisture state of rayon is attained when there is no measurable exchange of moisture between a volume of rayon and its surroundings. For rayon used under real-life conditions, it is doubtful when equilibrium is ever reached because the surrounding conditions are usually changing.[16]

Theoretically, the equilibrium moisture content of rayon at a specific temperature can be represented by a sorption isotherm. Sorption isotherms describe the relationship between the equilibrium moisture content of a material and the ambient relative humidity. Most materials exhibit sorption hysteresis; that is, desorption gives higher equilibrium moisture contents than adsorption at identical ambient climate conditions.[17]

The moisture sorption isotherms of natural fibers follow an International Union of Pure and Applied Chemistry (IUPAC) type II isotherm. A water sorption hysteresis, given by the difference between the sorption and desorption isotherms, is also observed.[10]

The equation 3 expresses the moisture content on a dry basis, that is, the mass percentage of water vapor on the dry adsorbent.[18]

$$moisture\ content\ (\%) = \frac{mass\ of\ sample - mass\ of\ dry\ sample}{mass\ of\ dry\ sample} \cdot 100\ \% \qquad (3)$$

2.3.5 Thermodynamics of the air moisture

A described in section 2.3.4, relative humidity to the amount of water vapor in the air, and it is used for the construction of the isotherms. Therefore, it is crucial to understand the meaning of relative humidity and how it varies with temperature, as well as, its relationship with absolute humidity.

Relative humidity, RH, is defined by the ration of the water vapor pressure (partial pressure), p_w, in a sample of moist air to the saturation water vapor pressure p_{ws} at the same temperature, expressed by equation 4.[19]

$$RH = \frac{p_w}{p_{ws}(T)} \cdot 100\ \% \tag{4}$$

The saturation water vapor pressure p_{ws} represents the amount of water that the air can hold at a certain temperature, and the water vapor pressure p_w indicates the actual amount of water that is held by the air. For example, at a relative humidity of 50 %, air contains only half of the maximum amount of water vapor it could hold at a specific temperature. At 100 % relative humidity, the air holds as much water as it possibly can, i.e. it is fully saturated with water vapor. If 100 % saturation is exceeded, the excess moisture precipitates as condensation.[20]

p_{ws} is a function of temperature; therefore, the relative humidity will also vary when temperature increases or decreases.

For a certain temperature (T), the saturation water vapor pressure can be calculated by equations 5 and 6 with enough accuracy for temperatures between 0 ˚C and 100 ˚C [22], as follows:

$$\vartheta = 1 - \frac{T}{T_c} \tag{5}$$

$$\ln\left(\frac{P_{WS}}{P_c}\right) = \frac{T_C}{T} \cdot (C_1\vartheta + C_2\vartheta^{1.5} + C_3\vartheta^3 + C_4\vartheta^{3.5} + C_5\vartheta^4 + C_6\vartheta^{7.5}) \tag{6}$$

Where T_c and P_c are, respectively, the critical temperature, in *K*, and critical pressure, in *hPa,* of the water and C_1, C_2, C_3, C_4, C_5 and C_6 constants that are given in Table 2.

Table 2: Coefficients defined for the calculation of saturation vapor pressure between 0 ˚C and 100 ˚C.[22]

Variable	*Value*
T_C	647.096 K
P_c	220640 hPa
C_1	-7.85951783
C_2	1.84408259
C_3	-11.7866497
C_4	22.6807411
C_5	-15.9618719
C_6	1.80122502

It is noticed by equation 6 that P_{WS}, increases with the rise of T. In other words, the capability of the air to hold water is raised for higher temperatures. According to equation 4, the increase of temperature leads to a lower relative humidity, for fixed amount of water vapor present in the atmosphere (P_W).

P_W can be related to the absolute humidity of the air (AH), which is defined as the mass of water vapor in a certain volume. If ideal gas behavior is assumed, AH is given in g/cm^3 and can be calculated using equation 7:

$$AH = C \cdot \frac{P_w}{T} \tag{7}$$

where $C = 2.16679$ g·K·J^{-1}, P_w is give n in Pa and T in K.

2.4 Rolling Resistance in Tires

The rolling resistance is one parameter to measure tire performance, and it is defined by the energy consumed by a tire per distance unit.[1] It can be responsible for up to approximately 20-30 % of the vehicle's total fuel consumption.[23] The energy loss is given by the hysteresis loop of the material stress-strain curve.[24] The hysteresis concepts and how to get parameters to predict the rolling resistance out of it are explained in the following sections.

2.4.1 Hysteresis

The hysteresis represents the history dependence of physical phenomena. Therefore, to observe the presence of hysteresis, a load is applied to the material, released and applied again. When hysteresis occurs, different responses are observed for the first and the second loading stages. This difference happens due to the energy dissipation of the material.[24] An example of a

hysteresis loop observed in Figure 8, where the result from the force-strain test for rayon cord material is displayed.

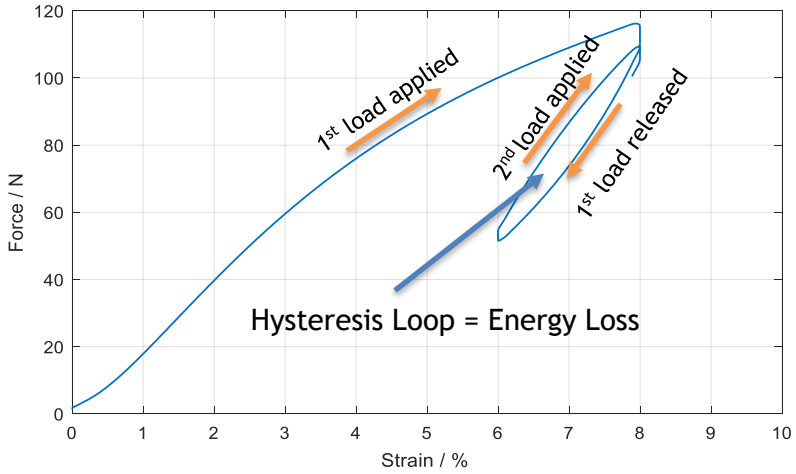

Figure 8: Example of a force-strain curve with hysteresis loop for rayon cords.

The hysteresis shows the tendency of a system to retain its properties in the absence of a load that generated them or is the ability to preserve a deformation made by the load. The more the materials retain its properties, the lower is the energy loss. The area of the hysteresis loop is represented by the energy dissipated per cycle.[25]

For this study, those load cycles can be translated as strain cycles. Strain is the change in the dimensions of a material compared to its original dimension. For the cord material, the tests are made in one dimension, and the strain, ε, is given by equation 8.

$$\varepsilon\ (\%) = \frac{\Delta l}{l_0} \cdot\ 100\ \% \tag{8}$$

Where Δl is the change in the length of the cord and l_0 is the original length of the cord.

2.4.2 Mechanical deformation of materials

The mechanical behavior of materials can be classified according to the tendency of recovering its deformation after applying and removing a load (Figure 9a), that is, the tendency of dissipating energy. The mechanical deformation is classified into elastic, viscoelastic and viscous.[26]

Pure elastic mechanical deformations show an ideal linear and instantaneous response according to the applied load. It fully recovers its deformation after the load is removed, therefore, the material returns to its initial dimension and hysteresis is not observed (Figure 9b).[26]

On the other hand, for a full viscous behavior, deformation or strain is not instantaneous; that is, in response to one applied stress, deformation is delayed or depend on time. Besides that, the deformation is not reversible after the release of the stress (Figure 9d).[26]

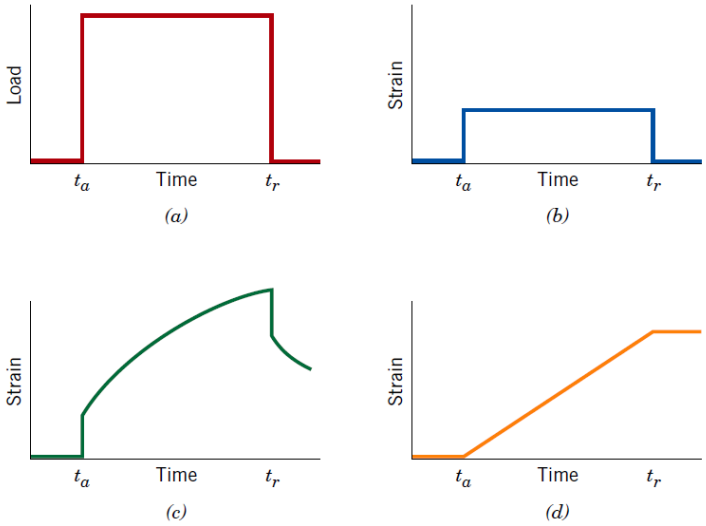

Figure 9: Representation of different mechanical responses to a load applied at time t_a and released at t_r.[26]

Viscoelastic responses show a combination of both effects; there is a viscous component and an elastic component. The imposition of stress results in an instantaneous elastic strain, which is followed by a viscous, time-dependent strain. After releasing the applied strain, only part of the deformation is recovered (Figure 9c).[26]

2.4.3 Dynamic Mechanical Analysis

Dynamic mechanical analysis (DMA) is a material technique which provides information on the material's bulk properties and thermal transitions. At frequencies and temperatures of interest, an oscillatory strain (or stress) is applied to the material, and the resulting stress (or strain) developed in the material is measured.[27]

The material strain and stress over time are given by the equations 8 and 9, respectively.

$$\varepsilon(t) = \varepsilon_0 \cdot \sin(\omega t) \tag{9}$$

$$\sigma(t) = \sigma_0 \cdot \sin(\omega t + \delta) \tag{10}$$

where ω is the frequency of the oscillatory applied stress, ε_0 and σ_0 the respective amplitudes and δ the phase shift between strain and stress.

When cyclic loading is applied to a material, the pure elastic component is displaced instantaneously with the load, while the displacement of the viscoelastic component is delayed as indicated by a phase shift (δ), showed in Figure 10. Thus, a phase shift of 0° indicates a purely elastic material, and an increasing phase shift corresponds to increasing viscoelastic character of

the material, up to a phase shift of 90°, indicating a purely viscous material. The DMA technique utilizes this phase shift to characterize the viscoelastic material.[28]

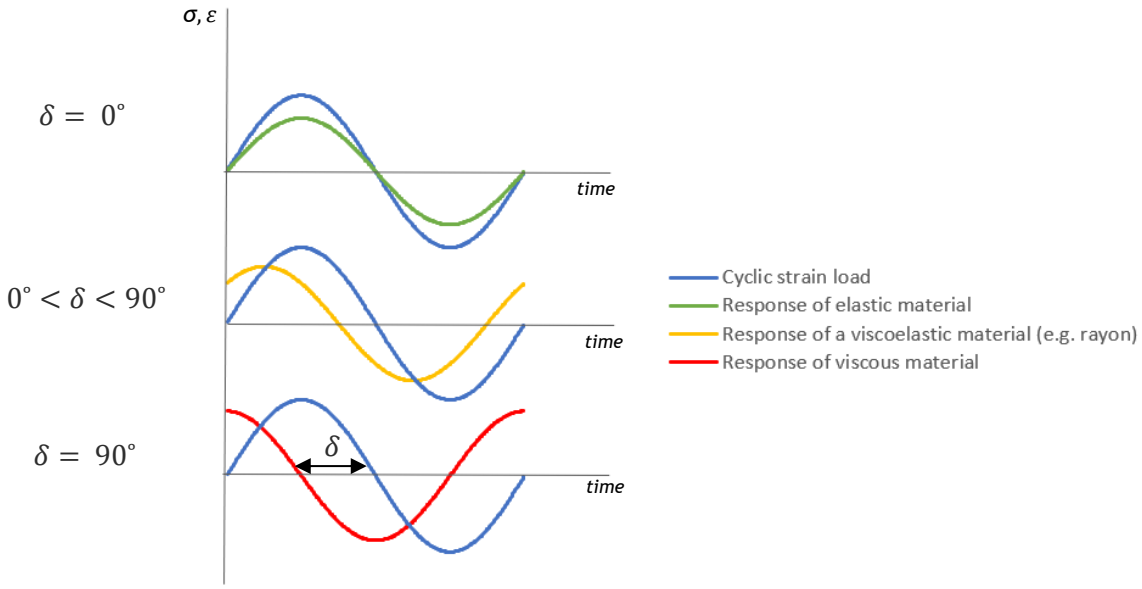

Figure 10: Mechanical response over time for an elastic, viscoelastic and viscous material after the application of an oscillatory load.

The phase shift occurs due to material damping.[28] The damping coefficient can be expressed as the tangent of the phase lag, tan δ, as follows:

$$\tan\delta = \frac{E''}{E'} \tag{11}$$

The elastic modulus (or storage modulus), E', is a measure of the recoverable stored strain. On the other hand, the viscous modulus (or loss modulus), E'', is a measure of the energy dissipated, generally lost as heat.[26,27] They are represented in equations (5) and (6), as follows:

$$E' = \frac{\sigma_0}{\varepsilon_0} \cdot \cos\delta \tag{12}$$

$$E'' = \frac{\sigma_0}{\varepsilon_0} \cdot \sin\delta \tag{13}$$

The characterization of viscoelastic materials done by DMA is used for quality control and product development purposes. The results are usually in the form of a graphical plot of E', E'', and tan δ as a function of temperature, frequency or time.[28]

3 Materials and Methods

3.1 Diffusion study of water molecules through cured and non-cured rubber.

In the first part of this thesis, a test method was developed to check if water vapor could penetrate through the rubber used in tires. For that, the hysteresis elongation of three different samples of rayon cords was evaluated: cured calendered cord, non-cured calendered cord and uncalendered cord (see Figure 13). The calendered samples were exposed to laboratory conditions for different time durations, and the mechanical properties were observed along the time.

3.1.1 Samples preparation

Uncured samples: the calendered rayon 1840x2 from the plant was used as uncured samples. It was previously stored at the laboratory with a protective material to avoid contact with moisture from the surrounding air. A skim compound was used for the calendering process of rayon fabric at the plant. A piece of material was cut using scissors and exposed to the controlled laboratory conditions (T = 23 ˚C and RH = 55 %), as showed in Figure 11 a.

Cured Samples: a part of the uncured samples was separated for the preparation of the cured ones. Firstly, the edges were closed with the same skim compound used during the calendering process, see Figure 11 b. The curing process was carried out in a high-pressure oven for 10-15 minutes, at 170 ˚C (see Figure 11 c). Finally, a rigid sample was formed and exposed to the same laboratory conditions (see Figure 11 d).

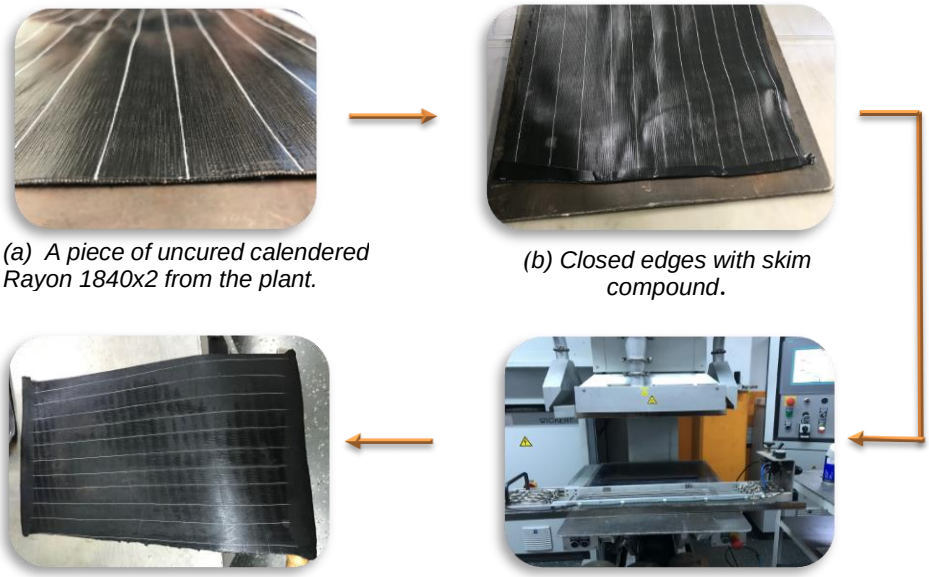

(a) A piece of uncured calendered Rayon 1840x2 from the plant.

(b) Closed edges with skim compound.

(d) Cured sample exposed to laboratory conditions.

(c) Curing process at 170 °C for 10-15 minutes in a high-pressure oven.

Figure 11: Preparation of cured and uncured calendered samples of rayon cords.

3.1.2 Procedure

The hysteresis elongation of cured and the uncured samples was evaluated at the Zwick/Roell Z005 Machine, presented in Figure 12. The samples laid on the table at the laboratory in order to uptake the water vapor present in the atmosphere. The samples were taken to be tested after different periods of exposure to the air, aiming to check how long time it would take to perceive an effect of moisture on the mechanical properties.

Figure 12: Representation of the Zwick/Roell Z005 machine used for hysteresis elongation tests.

After being prepared, the uncured samples were immediately tested, while the cured ones were tested only after one hour (after cooling down). Those samples represent the dry condition or reference. The next samples firstly laid on the table, before being tested, for the periods described in Table 3.

The hysteresis elongation of pure dry cords and saturated cords (for the same laboratory conditions) was also tested. Those results were used as a comparison to the ones from the calendered samples. Those saturated cords were taken from a fabric that was at the laboratory without storage conditions for a few weeks. The drying process of pure rayon cords was carried out at the oven (Memmert) for 1 hour, at 105 ˚C.

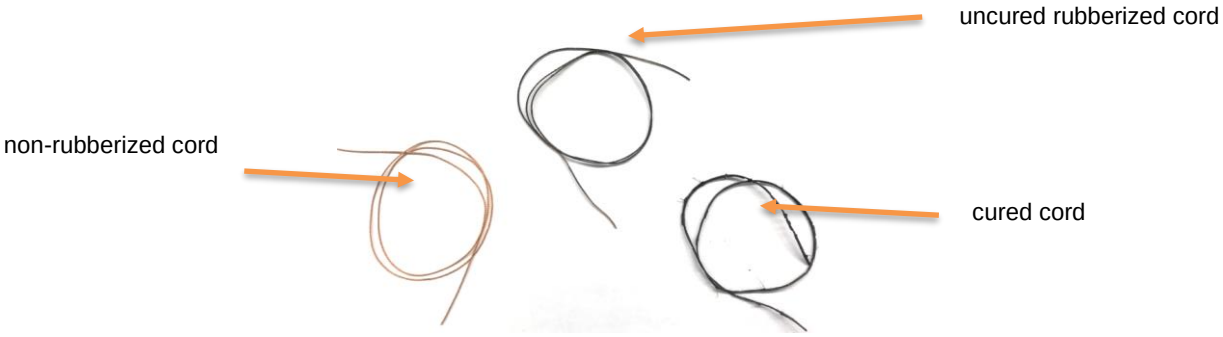

Figure 13: Example of cured, uncured, and pure rayon cords before being tested

The study hypothesis relied on the following: if the moisture does not achieve the cords within the rubber, the strain-stress curves of samples tested after long-time exposure to the air should look the same as the dry samples.

Table 3: Periods of exposure to the lab before being tested.

Period exposed to the lab before testing	Cured rubber	Uncured rubber	Pure cords
After preparation (Dry)	x	x	
1 Day	x	x	
2 Days	x	x	
3 Days	x	x	
4 Days	x	x	
2 weeks	x		
3 weeks	x		
No control (few weeks)			x

The sample length was approximately 400 mm, and the gauge length was 250 mm. A pre-load of 1.84 N was applied to the cord before the start of each test. The setup of the Zwick/Roell Z005 Machine included 100 cycles of oscillatory strain ranging from 6 to 8 %, at an elongation rate of 300 mm·min^{-1}.

The laboratory ambient conditions are controlled and kept constant. The parameters and conditions set in the machine during the test are showed in Table 4. The setup configuration and the data recording were done with the support of the software TestXpert II from the Zwick Machine. The data includes time in s, Force in N and strain in %. For the tensile strength and hysteresis behavior analysis, a graph is plotted showing the force on y-axis and the strain on x-axis.

Table 4: Parameters and specifications for the hysteresis elongation test.

Specifications for the test	
Material	Rayon 1840x2
Number of cycles	100
Strain range	6 to 8 %
Sample´s length	400 mm
Gauge length	250 mm
Elongation rate	300 mm·min^{-1}
Preload	1.84 N
Type of clamps	Parallel
Lab conditions	23 ˚C, RH 55 %
Number of samples	3

3.2 Investigation on the reversibility of rayon mechanical properties after its interaction with water

The hygroscopic behavior of cellulosic based materials, such as rayon, was described in section 2.3.1. It is known that the moisture will enter or release rayon cords according to the surrounding atmospheric conditions. On the other hand, it is unknown how the adsorption and desorption of water molecules affect the mechanical properties of rayon.

A new test method was developed to check if the force-elongation curves of dry rayon remain the same after the uptake and release of water or if a “memory effect” is observed. Finding it out is extremely important to ensure the reliability of the test methods developed in the following sections.

3.2.1 Set up of the procedure and samples preparation

The test consists of four cycles of heating and cooling rayon samples and evaluating the hysteresis elongation after each step at the Tensile machine (see Figure 12). Before the first heating step, the hysteresis elongation was also assessed to be used as a reference. In total, for each trial, the hysteresis elongation was evaluated at nine different steps, which are marked as circles in Figure 14. The red circles represent the heated conditions while the blue circles the cooled ones; yellow is the reference. Five trials were performed in order to check the reproducibility of the test.

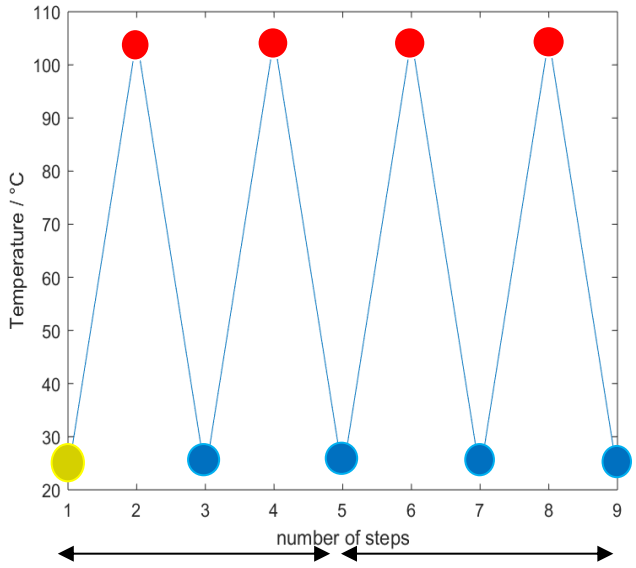

Figure 14: Scheme of the procedure.

The heating step was done by putting the samples into the oven for 1 hour at 105 ˚C. After that, the samples were exposed to the laboratory conditions (T = 23 ˚C and RH = 55 %) to cool down to room temperature. This step lasted two hours, which is time enough to achieve a moisture content close to the saturation value (see Annex A).

The testing material was rayon 1840x2, which was exposed to the lab atmosphere for a few weeks. Two long rayon cords (approx. 3 m) were taken from the fabric and cut into five pieces of length equal to 60 cm. This step was done to avoid deviations between the different cords present at the same fabric. The material used to perform the test are showed in Figure 16, while a scheme of the sample preparation is illustrated in Figure 15.

The first cord was used to evaluate cycles 1 and 2, while the second cord, to evaluate cycles 3 and 4. The reference was tested for both (step1). A loop was made in each piece to avoid a change in the twist of the cord, which can influence on the test results.

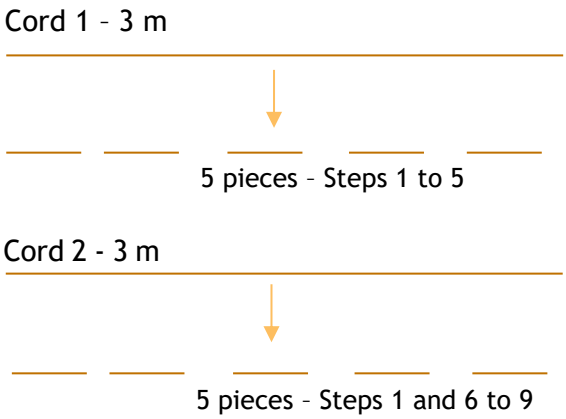

Figure 15: Scheme of the samples' preparation.

Figure 16: Materials used for the test.

One piece out of the five was separated to be tested as a reference, that is, under ambient conditions of the laboratory (T = 23 ˚C and RH = 55 %). The other four pieces were put onto an aluminum plate before being heated in the oven at 105 °C.

After heating, one piece of each sample was tested, and the others were exposed to the air at the laboratory for two hours. Following that, one of the cooled pieces was taken and tested, whereas the other pieces were put again into the same oven and same conditions. The previous steps were repeated until all the cycles were completed.

The process of taking the sample out of the oven, cutting the loop, putting the sample on the machine and closing clamping took around 45 s. This step should be done as quickly as possible because the water from the air interacts with rayon even when it is exposed for a few minutes (see Annex A).

The specifications at the Zwick Machine were the same as described in Table 4, except for the number of cycles, which were 10. That is because this test does not focus on a more in-depth study on the hysteresis behavior.

3.3 Development of the “iso-moisture” diagram

This section describes the methodology used to create the “iso-moisture” diagram presented in Figure 38. This diagram is nothing else but a two-dimensional (2D) plot in which each curve represents a contour line of equal moisture content of rayon at given conditions of temperature (x-axis) and relative humidity (y-axis). The data used to draw the diagram was obtained experimentally using thermogravimetric analysis (TGA). For each sample, the temperature was fixed, and relative humidity varied in order first to obtain the sorption isotherms of rayon described in section 2.3.4.

3.3.1 Thermogravimetric Analysis

Thermogravimetric analysis was performed to investigate the adsorption behavior of moisture in rayon samples under a controlled atmosphere. The tests were carried out at the TGA/DSC 2 from METTLER TOLEDO. The Modular Humidity Generator (MHG) from proUmid was attached to the TGA/DSC 2 for the humidity control. An example of those machines is presented in Figure 17.

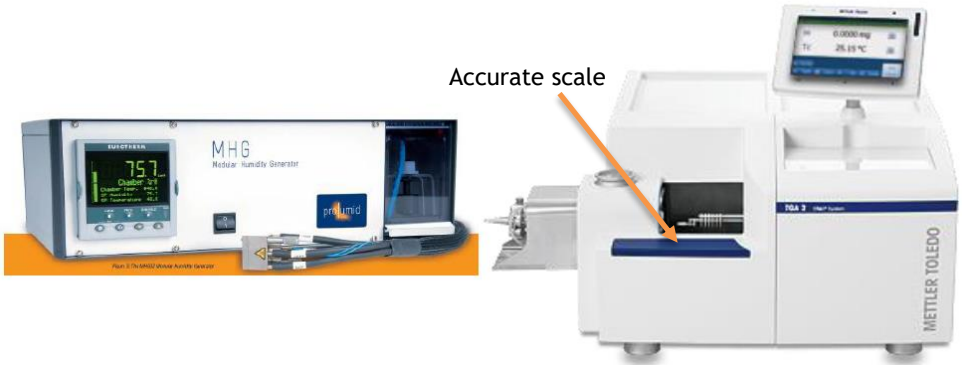

Figure 17: Example of the MHG (left) and the TGA/DSC 2 (right).

Figure 18: Samples of rayon cords in the pan, waiting to be placed on the furnace from TGA/DSC 2.

The tests consisted of monitoring the mass of rayon cords 1840x2 along time, while the sample specimen is exposed to a controlled temperature and relative humidity atmosphere. An example of TGA measurements is illustrated in Figure 19.

The sample is firstly placed on a pan, as showed in Figure 17. When the experiment starts, the pan is supported by a precision scale that resides in a furnace and is heated or cooled during the experiment. There is a flow rate of nitrogen gas to control the sample environment. The measured mass represents only the mass of the sample and not the pan. Because of that, the mass of the empty pan is required before the beginning of

each test. The scale XS105 Dualrange from Mettler Toledo was used to measured it. The length of the rayon cords samples was approximately 10 cm.

The temperature working range was limited due to the attachment of the humidity generator. The highest temperature should be 60 ˚C to avoid damage of the chamber and the lowest 20 ˚C. The relative humidity conditions had to be chosen in a way that dew point is not achieved. The working range of TGA is showed in Annex B. Each sample was tested at one chosen temperature, varying the relative humidity over time.

All samples were firstly dried at 60 ˚C and RH 0 %, for 180 min (at the same pan inside the TGA chamber). This step is observed by the decrease of the total mass. After that, the desired temperature and relative humidity to be studied are set up. Once the relative humidity is higher than zero, there will be water vapor around the rayon cord, and the textile will start to adsorb the water molecules. This is the mass uptake step, and it is observed with the increase of the total mass of the sample along time. The duration of the mass uptake was optimized, aiming to have a moisture content within the rayon as close as possible to the saturation conditions.

3.3.2 Conditions tested

The TGA study was based on the Ph.D. dissertation done at Continental by Hongying Zhao. Hongying Zhao studied the mass uptake of rayon cords over time using TGA, changing relative humidity, at a fixed temperature. Between each adjustment of relative humidity, the samples went through a drying step. Each mass uptake lasted 150 minutes, while the drying 40 minutes. Firstly, the raw data from his project was analyzed and the results are showed in Figure 19. Later, new conditions were carefully chosen to be tested and the setup was optimized in order to have a quicker test, as the thermo-gravimetric analysis is a time-consuming methodology.

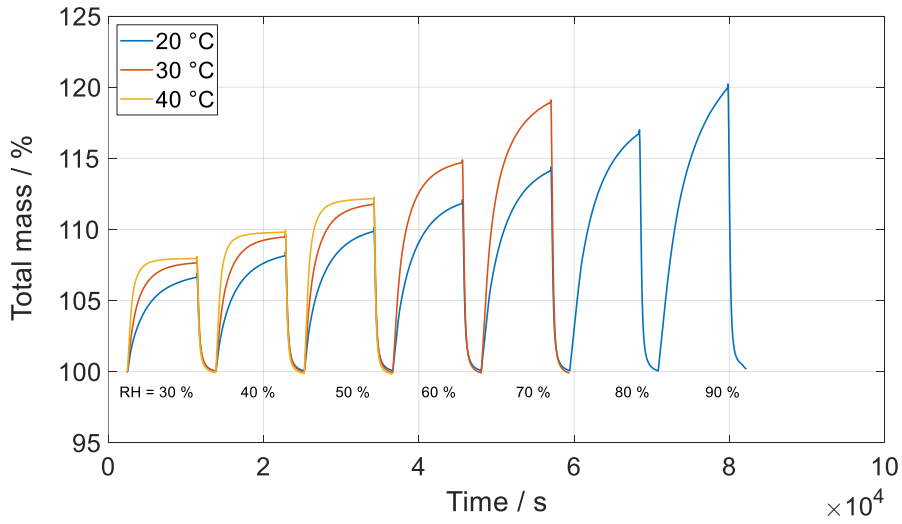

Figure 19: TGA measurements from Hongying Zhao.[30]

By looking at Figure 19, it is observed that the available data only includes results for relative humidity higher than 30 %, increasing in steps of 10 % up to the maximum *RH* value allowed by the machine, at temperatures 20 °C, 30 °C and 40 °C.

In order to have a broader range, it was decided to measure the mass uptake of rayon at RH 10 % and RH 20 % for temperatures: 20 °C, 30 °C, 40 °C, 50 °C and 60 °C. At higher temperatures, the dew point would have been achieved. Furthermore, for the optimization of the setup, the analysis at 30 °C was repeated.

The TGA/MHG atmosphere's setup conditions used by Hongying Zhao are showed in orange in Table 5, while the setup conditions used for the present master thesis are showed in grey. Both results are needed for drawing the "iso-moistures" diagram.

The configuration of the test procedure was done by two different software. The temperature over time was set up at the STARe Software from Mettler Toledo, whereas the relative humidity over time was established on the MHG Method Editor and MGH Control from proUmid.

Table 5: Previous and new conditions for measuring mass uptake of rayon cords using TGA.[30]

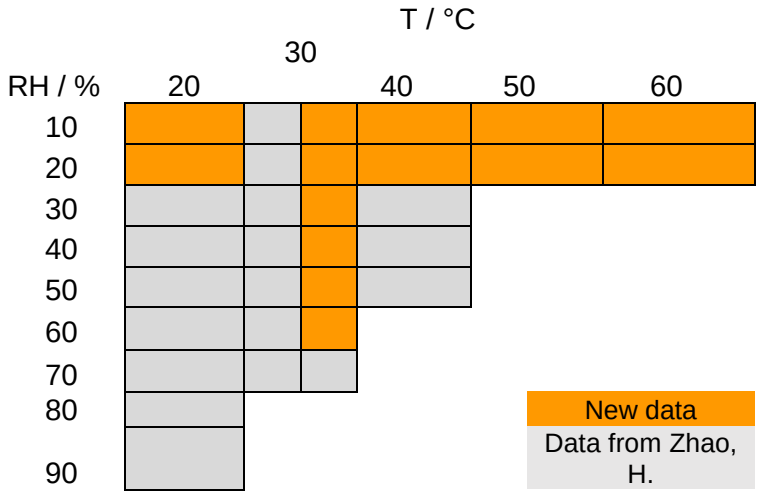

3.3.3 Setup optimization

The test method was improved along with the experiments, so the duration of the mass uptake step varied in order to optimize it. The testing conditions are presented in Table 6.

Test 1 and 2 followed the same procedure done by Hongying Zhao; that is, each mass uptake step lasted 150 minutes, having drying steps in between. From test 3, the period of the mass uptake step increased to 250 minutes as a tentative to achieve a moisture content closer to the saturation point. Test 3 was performed at 30 °C to compare with the results from Hongying Zhao, whether the moisture content was closer or not the saturation.

The question arises of course whether desorption of moisture during the measurements could influence the results. To answer that question, two tests were carried out at 40 °C; the first with the intermediate (test 4), and the second without the intermediate drying step (test 4). They

aimed to check if, in both cases, the rayon would achieve the same final moisture content. If so, the intermediate drying step could be removed, leading to a much shorter test.

The setup for each test should start with the lowest relative humidity to be tested and be increased after the time duration described in table 6.

Table 6: Specifications for the analysis done at TGA.

Test	Temp / °C	RH / %	Mass uptake duration / min	Drying step in between
1	20	10, 20	150	√
2	60	10, 20	150	√
3	30	10, 20, 30, 40, 50, 60, 70	250	√
4	40	10, 20	250	√
5	40	10, 20	250	X
6	50	10, 15, 20	150	X

3.3.4 Data analysis for the sorption isotherms drawing

The data from TGA and MHG were given in two different files. The first one provided the mass, set temperature and measured temperature over time, whereas the second one, the set relative humidity, and the measured relative humidity over time.

The mass was given in % or in mg, and it had to be normalized. The recording of the mass started together with the procedure, therefore, the pre-drying step was also recorded. The mass recorded at 180 min was used as *mass of dry sample* in equation (3), because that is the last value measured during the pre-drying step.

For the graph's representation, the mass was normalized to weight percentage, so the drying mass was 100 %. After the first 180 minutes, the mass uptake starts, the mass of the sample increases due to the moisture uptake up to the saturation value. The abscissa (X-axis) is displayed as time and the ordinate (Y-axis) as weight percent (%) or moisture content (%).

The goal of this section is to draw the isotherm graphs for the temperatures tested. For that, the saturation moisture content, which is the maximum amount of water vapor the rayon cord can adsorb, for given conditions of relative humidity and temperature, must be obtained. That would happen in time infinite, which is not experimentally practical. A scheme of how the TGA measurements are translated into sorption isotherms is illustrated in Figure 20.

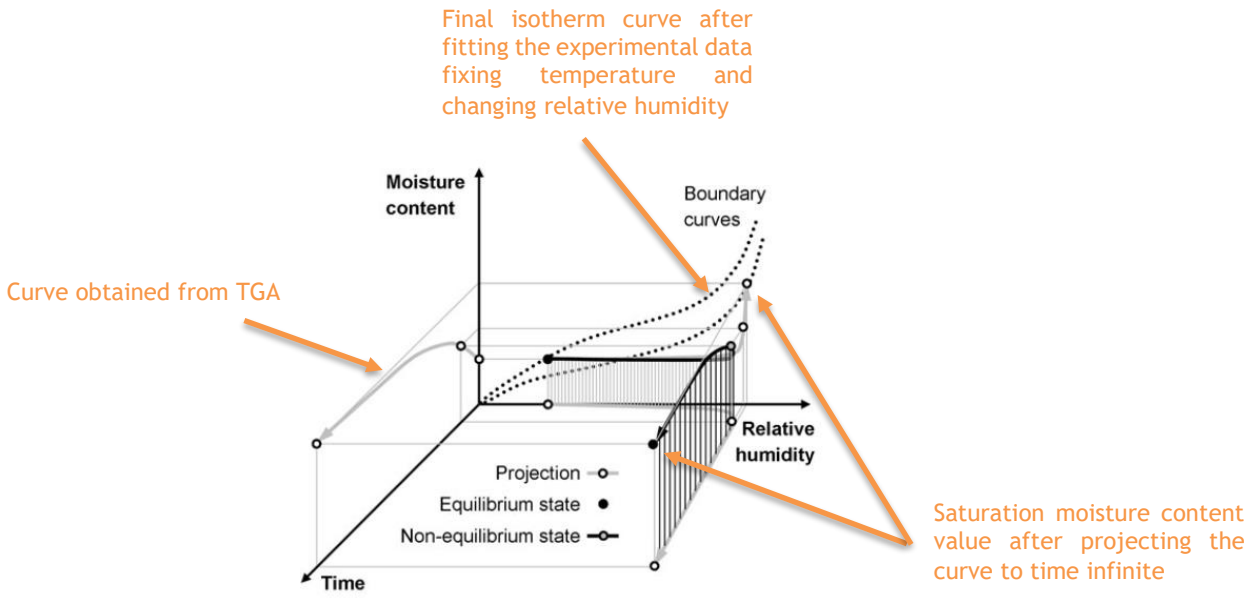

Figure 20: Schematic illustration of an adsorption process depicted in three-dimensional a moisture content–relative humidity–time domain. Adapted from reference 31.

The moisture content for time infinite was calculated by extrapolation of the last 2000 experimental values of measured mass during each mass uptake. The extrapolation was done with the support of the Curve Fitting Toolbox of MATLAB R2018a software, using equation 14.

$$MC\ (\%) = a * \exp^{\left(\frac{-t}{b}\right)} + c \qquad (14)$$

An example of starting point coefficients, as well as the lower and upper boundary conditions are showed in Figure 21.

The parameter c corresponds to the total mass of rayon at time infinite, the saturation value. From that, the saturation moisture content can be calculated using equation (3).

The same procedure is done for all the testing conditions mentioned in table 5. Three diagrams are derived from that data: the rayon isotherms, the three dimensional (3D) $MCxTxRH$, and the “iso-moistures”.

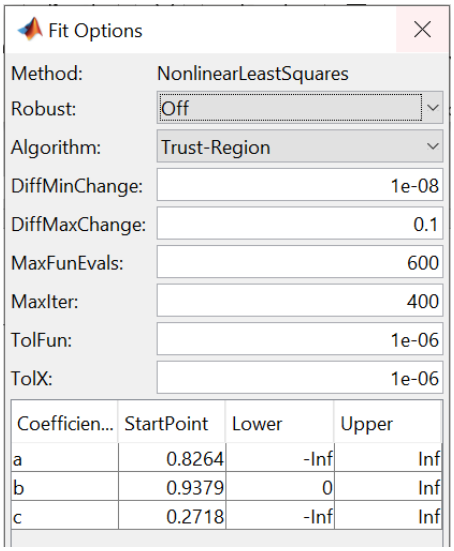

Figure 21: Example of starting point coefficients for fitting.

3.4 Static and dynamic response of rayon cords under controlled conditions

The MTS Acumen^{TM} 3 Test System connected to the MTS Flextest 40 Controller was used to perform dynamic (high frequency) and static (low frequency) response of rayon cords. The Mytron KPK 27 KH Climate Chamber was used in order to control temperature and humidity during the tests. The software MultiPurpose Testware (MPT) and the MultiPurpose Elite (MPE) were used for the test procedure creation and for the data acquisition throughout the test. The machine configuration is showed in Figure 22.

Figure 22: The final configuration of the MTS Acumen^{TM} 3 Test System connected to the controller and the chamber.

3.4.1 Validation of the "iso-moisture" diagram through static response

A new test method was developed to validate the "iso-moisture" diagram displayed in Figure 38. That is, to validate if one "iso-moisture" curve indeed represents the atmospheric conditions (RH and T) which lead to a constant saturation moisture content within rayon cords.

In sections 4.1 and 4.2, it was learned that the presence of moisture content in rayon cords changes the material stiffness substantially, and that can be perceived throughout tensile-strength tests. Based on that, the hysteresis elongation test was performed at different atmospheric

conditions, which were chosen following the same “iso-moisture” line. If the moisture content is indeed the same for the different atmospheres, the hysteresis elongation curves should overlap.

Although the tensile-strength tests of textiles are typically performed at the Zwick/Roell machines (e.g. Figure 12), the MTS configuration, displayed in Figure 22, was chosen due to the possibility to control the relative humidity and the temperature at the chamber attached to it.

All the samples of rayon cords were previously dried for one hour at 105 ˚C in the oven. The relative humidity and the temperature of the chamber were adjusted to the ones specified in Table 7. After that, the sample was clamped in the MTS machine using pneumatic clamps and remained for two hours before the test started. The waiting period of two hours is long enough to achieve a moisture content close to the saturation value (see Annex A).

Table 7: Specifications for three tests done for the validation of the “iso-moisture” diagram.

Test 1 - Rayon 1840x2			
	MC / %	Temperature / ˚C	Relative Humidity / %
Sample 1	12.5	40	50
Sample 2	12.5	20	60
Test 2 – Rayon 1840x2			
	MC / %	Temperature / ˚C	Relative Humidity / %
Sample 1	8	20	40
Sample 2	8	30	30
Sample 3	8	40	**30**
Test 3 - Rayon 2440x2			
	MC / %	Temperature / ˚C	Relative Humidity / %
Sample 1	8	30	30
Sample 2	8	20	40

Firstly, samples of rayon 1840x2 were tested fixing moisture content at 12.5 % for two different controlled atmospheric conditions: the first one setting the chamber to T = 40 ˚C and RH = 50 %, while the second one T = 20 ˚C and RH = 40 %.

Later, the moisture content of 8 % was chosen in order to check the behavior for a lower range of relative humidity. Three different conditions were taken: T = 20 ˚C, RH = 40 %; T = 30 ˚C, RH = 30 % and T = 40 ˚C, RH = 30 %.

As described in section 3.3, the “iso-moisture” diagram was developed from TGA measurements of rayon 1840x2. To investigate if the diagram could also be applied to rayon 2440x2 (thicker rayon cord), the same conditions of the first test (*MC* fixed at 12.5 %) were applied to that material.

The specifications for the hysteresis elongation test, presented in Table 8, include a preload of 1.84 N; gauge length of 100 mm; a strain rate of 120 mm·min^{-1}, ranging the strain from 8 to 10 %, for 100 cycles.

Table 8: Specifications for the hysteresis elongation tests at the MTS.

Name	Value
Number of cycles	100
Strain range	6 to 8 %
Sample´s length	500 mm
Gauge length	100 mm
Elongation rate	120 mm·min^{-1}
Preload	1.84 N
Type of clamps	Pneumatic

3.4.2 Dynamic mechanical analysis of rayon cords

This section aims to characterize the viscoelastic behavior of rayon cord material through dynamic mechanical analysis. The dynamic response is observed for the application of sinusoidal strain at different frequencies and temperatures. The MTS Acumen 3 Test System was used to perform the tests.

Firstly, a skim compound was added to the tips of the cord (where it will be in contact with the clamps) to avoid slippage and friction. Later, the samples went through a curing process, which carried out in the high-pressure oven at 170 ˚C for 10 minutes. An example of the prepared sample is showed in Figure 23.

Figure 23: Example of a sample of rayon cord prepared for the dynamic mechanical analysis.

After the vulcanization, the samples were exposed to the lab; therefore, the spontaneous mass uptake of water started. Because of that, before each test, the samples were dried in the oven for one hour at 105 ˚C. The temperature in the chamber was set to 25 ˚C, in a ramp rate of 3 ˚C·min^{-1}, which is the lowest temperature to be tested.

The relative humidity of the chamber was set to 10 %. This value was chosen for the two following reasons. First, according to the “iso-moisture” diagram (see Figure 38), the saturation moisture content of rayon is almost constant for low relative humidity. Second, for the chosen temperature working range, RH = 10 % is the lowest value allowed by the configuration of the chamber.

The procedure started by clamping the sample using pneumatic clamps, followed by the application of the preload of 1.84 N. After that, there was a pre-step of sample conditioning which consisted of applying ten cycles of sinusoidal strain ranging from 1 % to 5 %, at 120 mm·min^{-1}, in order to pre-damage the sample and exclude this effect from the dynamic response.

Finally, the dynamic test was performed by applying a sinusoidal strain, ranging from 4 % to 6 %, at 20 Hz for one hour. After the end of this step, the temperature was kept constant and equal to 25 ˚C, and a lower frequency of 10 Hz was applied. Following that, the frequencies 5, 2, 1, 0.3 and 0.1 Hz were respectively applied.

The next step consisted of increasing the temperature of the chamber to 40 ˚C, waiting two hours for the mass uptake step and applying the same frequencies to the sample. The same is performed at 55, 70 and 85 ˚C. The data acquisition system monitors the stress and strain over time, which will be used to calculate the parameters needed for the viscoelastic characterization of the material, that is, E', E'' and tan δ described in section 2.4.3.

4 Results and Discussion

The chapter is divided into four sections, each one discusses the results from the four different investigation in which the test procedures were described in Chapter 3.

4.1 Diffusion study of water molecules through cured and non-cured rubber.

It is known that cellulose-based materials uptake water molecules from the air due to its hygroscopicity. The increase of water content has an impact on the material stiffness. Dry rayon cords are stiffer than “wet” ones (see Annex A). On the other hand, the rayon cords present in tires are surrounded by a skim compound, therefore, it is questionable if the rubber should avoid the water uptake.

To answer this question, a new test method was developed and presented in section 3.1. The variation of the stiffness due to the presence of water can be used as an indicator of adsorption of vapor molecules by rayon cords. The water adsorption by calendered rayon (textile + rubber) was studied at two different cases: having the cord embedded by cured and uncured rubber.

Samples of cured and uncured rayon cords were prepared as described in section 3.1.2. The samples were exposed to the lab atmosphere (T = 23 ˚C and RH = 55 %) for different periods, as described in Table 3. The hysteresis elongation test was performed after those periods of exposure to the air in order to check if the material stiffness would vary along with time, which would indicate the presence of water molecules. The force-strain diagram including the hysteresis loops is showed in Figure 24 for the uncured samples and in Figure 25 for the cured ones.

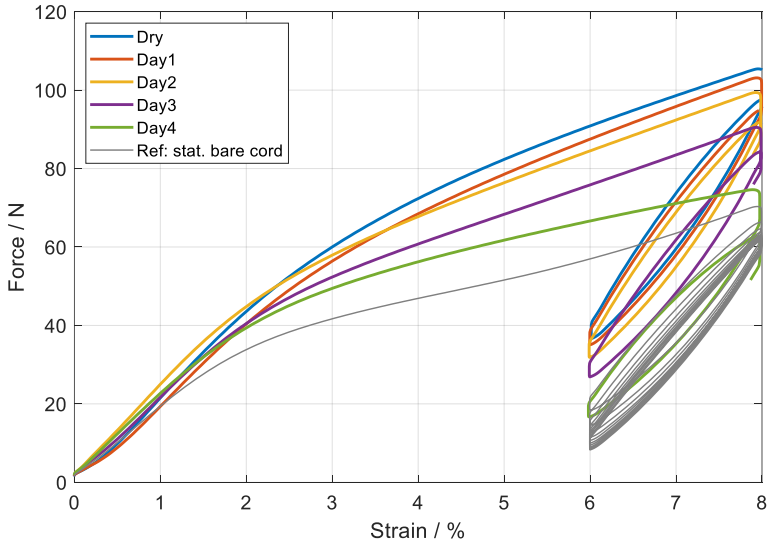

Figure 24: Force-strain curve with hysteresis loop over time of uncured rubberized rayon 1840x2.

The cord was elongated up to 8 % of its initial length, released back to 6 % and elongated again to 8 %, as seen in Figures 24 and 25. The last two steps were repeated for 100 cycles in order to have data for a future hysteresis behavior study. Only the first hysteresis loop is exhibited for easier visualization, as the main goal is to analyze the change in the material stiffness over time.

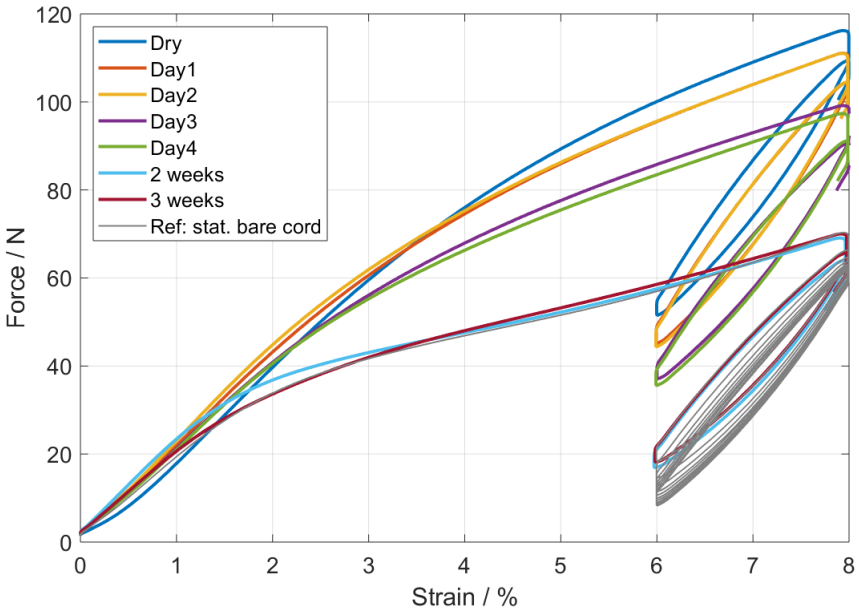

Figure 25: Force-strain curves with hysteresis loop over time of cured rayon 1840x2.

In both diagrams, the blue line shows the highest stiffness, that is expected because it is the dry condition. It is important to note that the dry uncured sample does not mean the sample went through a drying process. It represents the sample tested as soon as the material was removed from the storage. On the other hand, the dry cured samples were tested 1 hour after the curing process.

Comparing both dry conditions at the cured and uncured diagram, it is noticed that the force achieves, in the first elongation, around 115 N for the cured sample and 105 N for the uncured one. This difference is due to a few water molecules that were present at the uncured material when stored. It shows that the protective material wrapped around the calendered rayon does not block the water vapor completely.

The stiffness of rayon cords drops over time at both diagrams, which means that water molecules do penetrate through the rubber used in the rayon calendering process. For the uncured samples, the decrease is perceived within the first days, whereas for the cured samples in the first weeks. It is conclusive that the rubber delays the adsorption phenomena of vapor molecules into rayon cords but does not avoid it.

Bare rayon cords that were exposed to the lab for few weeks were also tested. Those cords were fully saturated with water vapor. The hysteresis elongation of a pure cord is included on both diagrams as a reference, plotted in gray. It shows how soft the material can become when present at the same surrounding lab atmosphere (T = 23 ˚C and RH = 55 %) for enough time.

Figure 24 shows that uncured samples are close to saturation conditions after 4 days, while Figure 25 reveals that saturation of cured samples is achieve after 2 weeks. Normally, the saturation of a bare cord occurs in approximately two hours (see Annex A). The longer delay perceived in the cured samples can be explained by the curing process. During the vulcanization, cross-links between the polymers chain are formed, leading to a higher rigidity of the material, which makes the water diffusion slower.

Both diagrams also reveal that the effect of moisture content is observed only for stretches greater than 1.5 %; therefore, humidity is not a problem for applications where the rayon cord strain is below this value.

4.2 Investigation on the reversibility of rayon mechanical properties after its interaction with water

As mentioned before, dry rayon has the ability of adsorbing water from the air until the equilibrium is established. Section 4.1 proved that even rubber-covered rayon becomes softer in the presence of moist air. Because tires have the same configuration (textile + rubber) in the manufacturing process, there is a high motivation for a deeper understanding of this topic.

According to section 4.1, rayon presents the highest tensile strength at dry conditions and the softest at the saturation conditions. No study in literature was found about how the rayon mechanical response is, when it goes through consecutive heating and cooling processes.

A new test method was developed and described in section 3.2 to evaluate the stiffness behavior of rayon cords after four successive cycles of heating and cooling. As described in the procedure, two different long cords (each one divided into five pieces) were used to perform each trial. The first cord went through the two first cycles and the second one through the third and fourth cycle. The force-strain curves with the hysteresis loops of rayon 1840x2 after carried out in the first and second cycles of heating and cooling are presented in Figures 26, whereas the same is showed in Figure 27 for the tests performed after the third and fourth cycles.

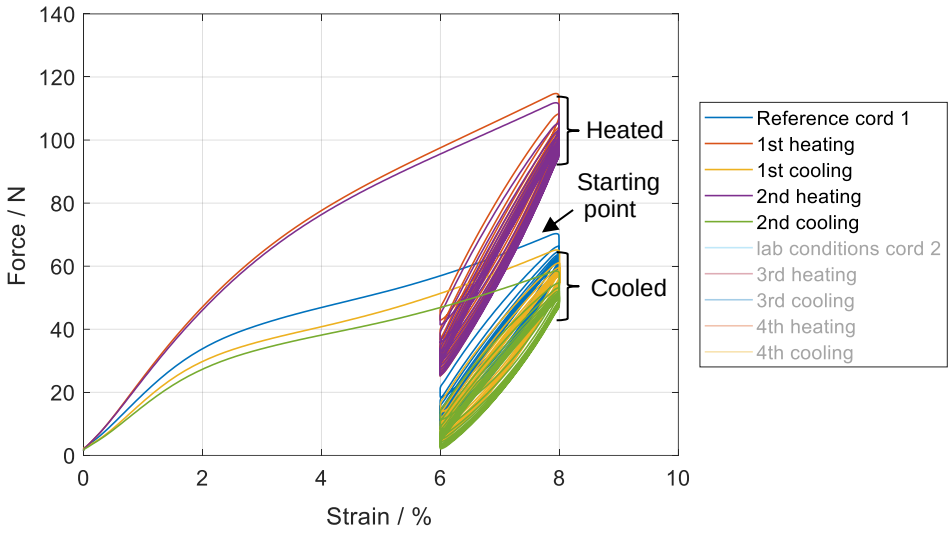

Figure 26: Force-strain diagram with hysteresis loop of rayon 1840x2 after 1 and 2 cycles of heating and cooling and the reference.

The reference, that is, the saturated cords before heated for the first time, are also tested and displayed in Figures 26 and 27 by the blue curves. The reference is the starting points and the other curves are compared to this one, as there is some deviation from cord to cord. As expected, the force-strain curves show much higher stiffness at dried conditions in comparison to the cooled conditions due to the presence of water molecules within the textile. The two diagrams show that the force-strain curves are fully recovered after being heated, going back to its maximum force. On the other hand, the saturated cords present a drop in the tensile strength of roughly 5 N after each cycle up to the third cycle, from when it stays constant.

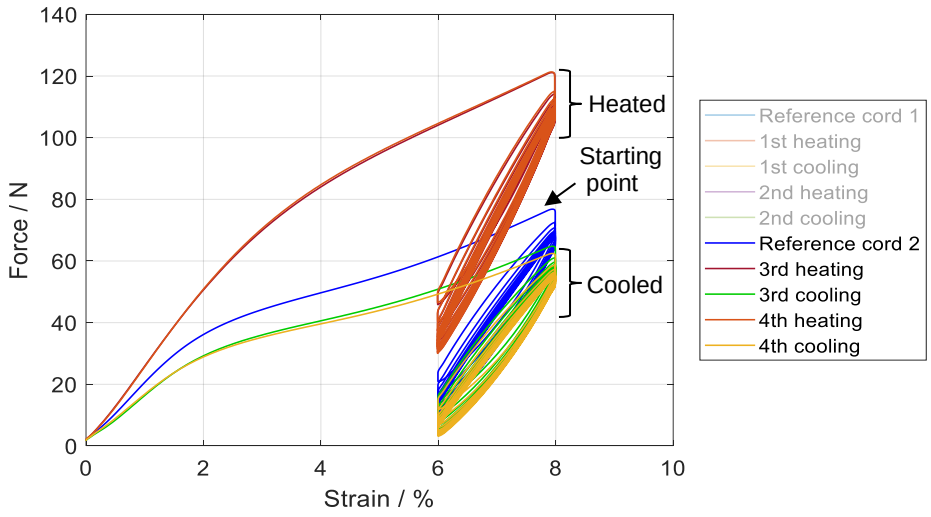

Figure 27: Force-strain diagram with hysteresis loop of rayon 1840x2 after 3 and 4 cycles of heating and cooling and the reference.

4.3 Development of the isotherm curves

4.3.1 TGA measurements and interpretation

Section 4.1 proved that even calendered rayon adsorbs moisture from the air, leading to a material softening. Section 4.2 verified that stiffness of dry rayon is recovered after successive cycles of water vapor adsorption and desorption. Those two sections investigated rayon behavior under one specific atmosphere, T = 23 ˚C and RH = 55 %. Those are the controlled conditions at the laboratory where the tests were performed.

If the test had been performed in another laboratory or another country with a different atmosphere, the tensile strength given by the force-strain curves would be altered. That occurs due to change on the moisture content of rayon cords, which is given by the equilibrium with the water vapor molecules present in the surrounding atmosphere

The mechanical properties of rayon material are intimately bonded to its moisture content; therefore, the prediction of the last one at different atmospheric conditions is crucial to the development of new test methods regarding this textile.

This section investigated the saturation moisture content of rayon under different atmospheric conditions of temperature and relative humidity. Thermo-gravimetric analysis was performed in order to monitor the water uptake of rayon by measuring the change of its total mass over time.

The different atmospheric conditions performed at TGA were presented in Table 6 in section 3.3.3. The results from test 1 and 2 are illustrated in Figure 28. The two curves show the variation of the total mass of rayon over time, at 20 ˚C and 60 ˚C. The procedure at 60 ˚C was not performed as expected, as the machine achieved only RH = 15 % instead of RH = 20 %.

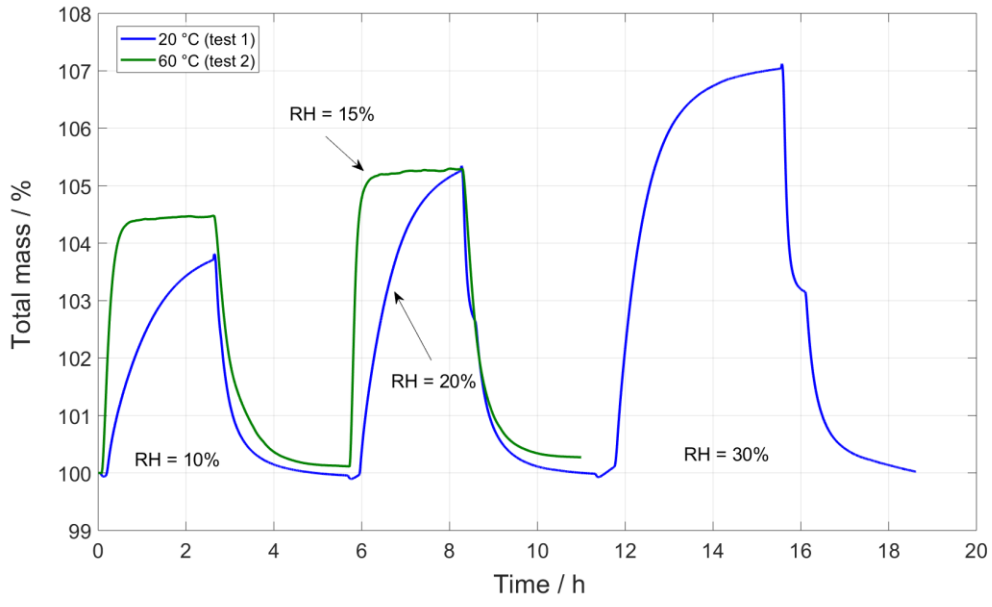

Figure 28: TGA curves for rayon 1840x2 performed at 20 ˚C and 60 ˚C.

In the beginning, each sample had a total mass equal to 100 %, which means the sample was dry. The relative humidity was changed from 0 % to 10 %, and water vapor was then added to the surrounding air. So, the mass uptake began, together with the increase of the total mass. After 150 minutes, the drying process started (T = 60 ˚C and RH = 0 %), aiming to remove all the water molecules from the sample. This step lasted 180 min, and another mass uptake step followed it. These consecutive cycles of desorption and adsorption of water vapor molecules are done until all the testing conditions are evaluated, at a specific temperature.

Overall, the moisture content grows with the increase of relative humidity, at a fixed temperature. That occurs owing to the fact that for higher relative humidity values and fixed temperature, there are more water molecules available in the air to be adorbed by the rayon sample(equation 10).

Another effect is noticed when the *RH* is fixed, and different temperatures are compared. For instance, by looking at both curves at fixed *RH* = 10 %, the moisture content is higher at 60 ˚C. That is explained by the thermodynamics of the air moisture (details in section 2.3.5). The saturation water pressure increases with temperature, which means the air capacity to hold water molecules is elevate; therefore, RH decreases according to equation 10. In order to keep RH constant, the absolute humidity must be altered. As a result, the concentration of water vapor in the air, or the absolute humidity, is higher at 60 ˚C than at 20 ˚C; hence, the equilibrium is shifted towards adsorption.

At the 60 ˚C curve, a stable plateau after the end of each mass uptake step is noticed, meaning rayon reached the saturation moisture content. On the other hand, the tendency of mass growth is clear at 20 ˚C, showing that the test could have lasted longer to achieve saturation state. Thus, it is conclusive, therefore, that the adsorption kinetics is favorable with the increase in temperature.

4.3.2 Optimization of the procedure

The TGA is a high timing-consuming analysis, therefore, an optimization of the procedure was proposed. According to the precedent section, the mass uptake is slower when the test is performed at lower temperatures. Based on that, tests 3 and 4, which were carried out at temperatures 30 ˚C and 40 ˚C, respectively, had a longer mass uptake step, which lasted 250 minutes instead of 150 minutes, in order to have moisture content closer to the saturation. The results from tests 3 and 4 are presented in Figure 29.

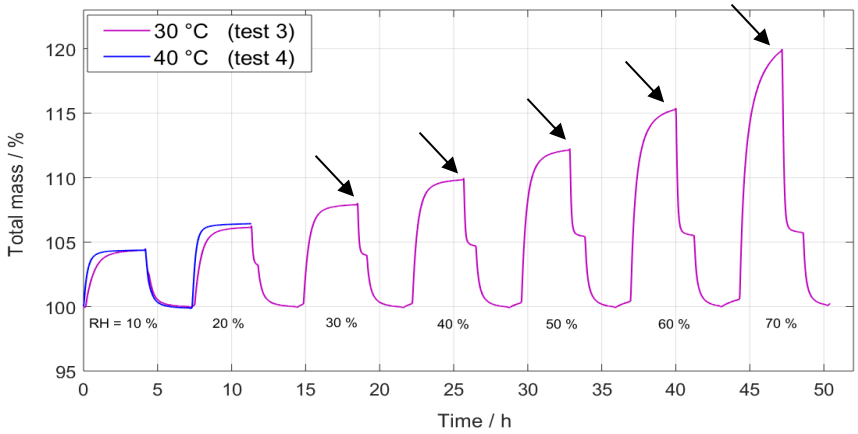

Figure 29: TGA curves from rayon 1840x2 at 30 ˚C and 40 ˚C.

The last value of some mass uptake step performed at 30 ˚C (marked by the black arrow in Figure 29) was taken out and compared to the ones obtained by Hongying Zhao. The total mass from the test carried out at the longer step achieved a value of approximately 3 % higher than at the shorter one. This increase is not significant enough to justify a more lengthy procedure.

Tests 4 and 5 aimed to answer whether desorption of moisture during the measurements could influence the results. They had the same specifications, except for the drying step in between the mass uptake, which was removed in Test 5. The results for tests 4 and 5 are showed in Figures 30 and 31, respectively.

The difference between the final mass value between the two tests was around 1.5 %; that is low and within the experimental error range. Because of that, it was concluded that moisture desorption does not influence the final result. Hence, the optimized procedure excludes the intermediate drying steps, having a shorter duration.

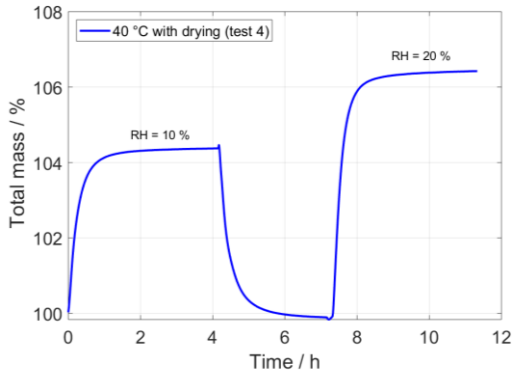

Figure 30: TGA curve for rayon at 50 ˚C with intermediate drying step.

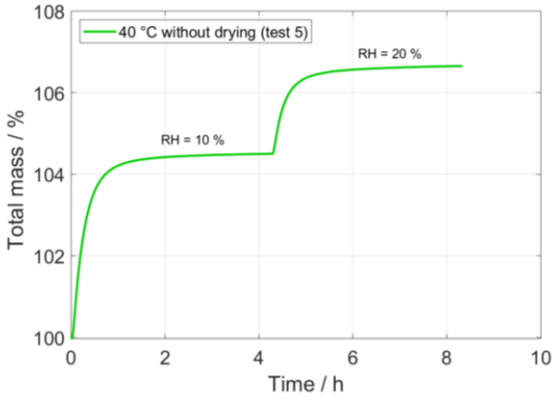

Figure 31: TGA curve for rayon at 50 ˚C without intermediate drying step.

Test 6 was carried out at 50 ˚C with optimized conditions. That is, pre-step of drying at 60 ˚C for 180 minutes, followed by successive mass uptake steps of 150 min, without intermediate drying steps in between. The result is showed in Figure 32.

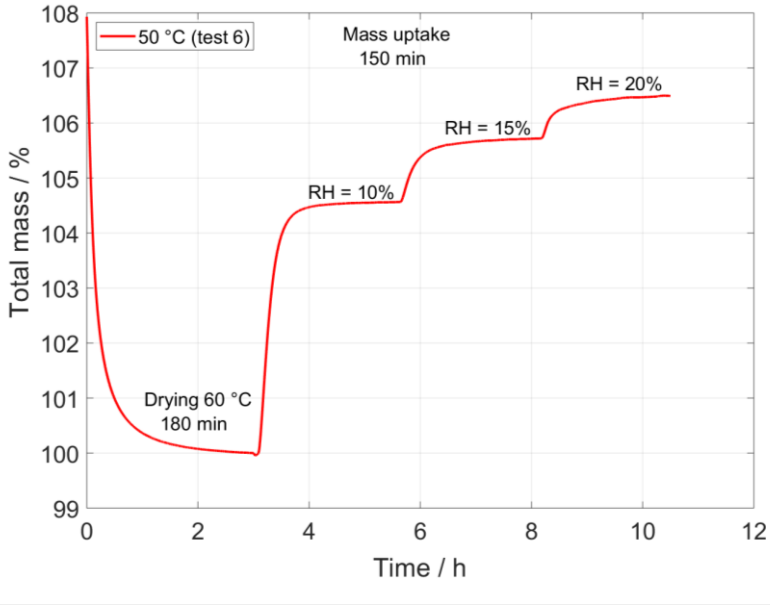

Figure 32: TGA measurements of water sorption by rayon; carried out at optimized procedure.

4.3.3 Estimation of saturation moisture content of rayon cords

The TGA measurements aimed to obtain the saturation moisture content of rayon at different atmospheric conditions, to be then used for drawing the sorption isotherms of this textile. The saturation moisture content is found when the concentration of water vapor within the solid reaches the equilibrium with the concentration of water vapor in the air. In other words, the saturation moisture content is the maximum weight percentage of water that can be found in rayon, when exposed to a certain atmosphere.

The outcome curves from TGA, which were initially given in total mass, were firstly converted to moisture content over time; an example is showed in Figure 33. The last and highest moisture content value measured for each atmosphere was taken (marked by the black arrows in Figures 29 and 33) and presented in Table 9. That is because those values are the closest to the saturation condition. They are plotted over relative humidity and presented in Figure 34.

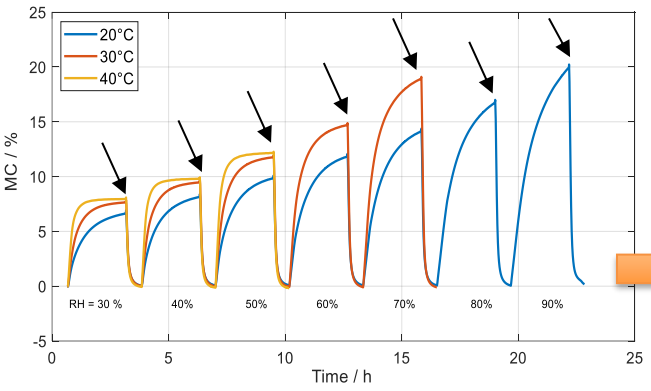

Figure 33: Example of TGA curves used to estimate the rayon sorption isotherm.

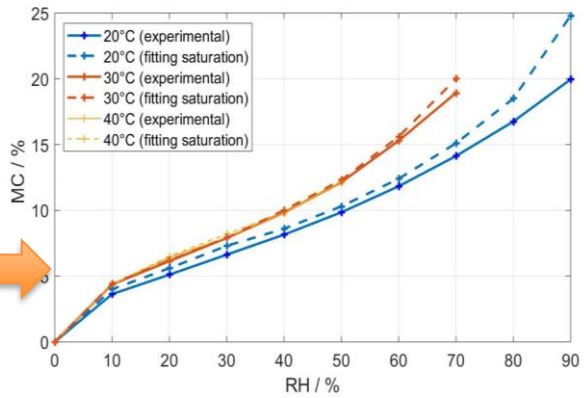

Figure 34: Experimental and extrapolated curves of moisture content over relative humidity, fixing temperature.

Table 9: Experimental moisture content of rayon cords under different atmospheres.

	Moisture content in dry-basis / %				
T / °C RH / %	20	30	40	50	60
0	0	0	0	0	0
10	3.6	4.4	4.4	4.6	5.1
20	5.1	6.1	6.4	6.5	
30	6.6	7.6	8.0		
40	8.1	9.5	9.8		
50	9.9	11.8	12.1		
60	11.8	12.7			
70	14.4	18.9			
80	16.5				
90	20.0				

New Data
Data from H. Zhao

For most of the analyses, the moisture content from Table 9 does not represent the equilibrium state or the saturation because the TGA did not run long enough for that. A curve-fitting procedure was done to predict the moisture content at time infinite, in other words, to predict the saturation moisture content. The curves are fitted using equation (14), following the procedure described in section 3.3.4. The extrapolation was done for all the TGA testing conditions, which were presented in Table 5 in section 3.3.2 and the results are presented in Table 10.

Table 10: Saturation moisture content of rayon cords under different atmospheres, calculated by fitting equation (14).

	Saturation moisture content in dry-basis / %				
T / °C RH / %	20	30	40	50	60
0	0	0	0	0	0
10	4.0	4.4	4.4	4.6	5.1
20	5.6	6.2	6.5	6.8	
30	7.3	7.7	8.2		
40	8.6	8.6	9.9		
50	10.3	12.0	12.2		
60	12.4	15.1			
70	15.1	20.0			
80	18.5				
90	24.8				

New Data
Data from H. Zhao

Both the experimental and the extrapolated moisture content were plotted over relative humidity and displayed in Figure 32. The first one is given by the solid lines whereas the second one by the dashed lines. The data used for the plotting comes from the curves illustrated in Figure 29 and are presented in table 9 and 10, from temperature ranging from 20 ˚C to 40 ˚C and RH from 30 % to 90 %. The extrapolation values are higher than the measured valued as expected. This difference is more noticed for the 20 ˚C curve and for relative humidity higher than 60 %. By this comparison, it has been proven, therefore, the importance of using the fitting equation.

4.3.4 Sorption isotherms of rayon cords

All the extrapolated moisture content, presented in Table 10, are also plotted over relative humidity, fixing the temperature and illustrated in Figure 35. Each curve is a sorption isotherm of rayon cords (details in section 2.3.4). In other words, each curve shows the moisture content of rayon when it is in equilibrium to the surrounding air. The curves are shorter for higher temperatures to avoid dew point conditions at the TGA machine.

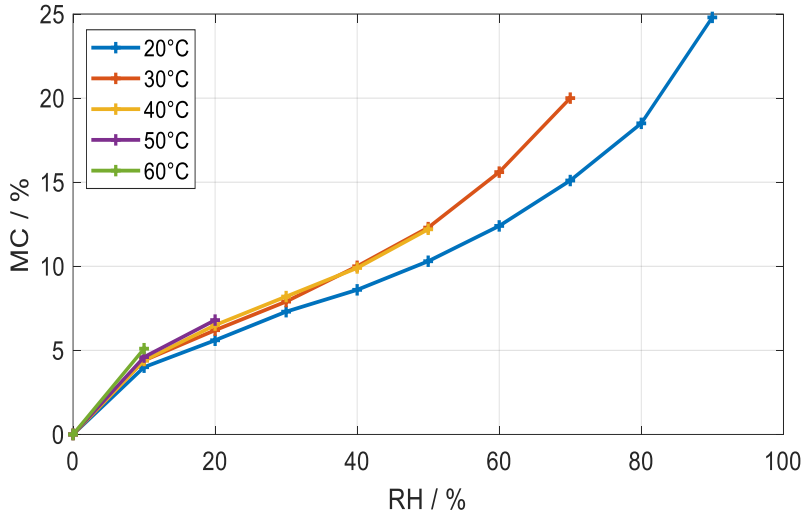

Figure 35: Sorption isotherms of rayon cords.

The sorption isotherm curves from in Figure 35 can be represented over absolute humidity as well. The relative humidity was converted into absolute humidity following the equations described in section 2.3.5. The moisture content over absolute humidity is showed in Figure 36. When the concentration of moisture in the air is fixed (AH constant), the moisture content drops with the increase of temperature, proving the exothermic behavior of the adsorption process.

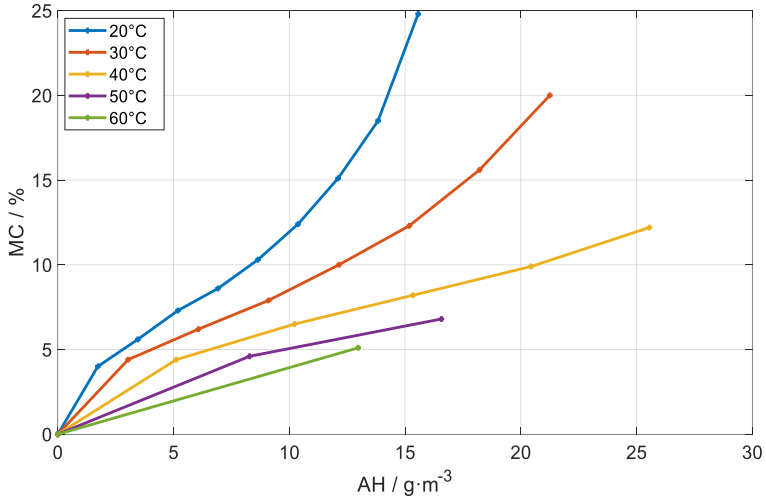

Figure 36: Saturation moisture content of rayon over absolute humidity, at different temperatures.

4.3.5 Creating the "iso-moisture" map

The main goal of section 4.3 was to develop the "iso-moisture" diagram and that involved some pre-steps. Firstly, the $MCxTxRH$ diagram was drawn by taking the saturation moisture content of rayon cords at different conditions of temperature and relative humidity. This diagram a three-dimensional (3D) plot which relates the saturation moisture content of rayon (z-axis) at given conditions of temperature (x-axis) and relative humidity (y-axis). The diagram was plotted in MATLAB using the data from Table 10 and it is presented in Figure 37.

The black dots show the values taken from Table 10 while the entire curve was extrapolated using the Fitting Tool from MATLAB. This diagram enables one to easily perceive how the atmospheric conditions have a significant impact on the saturation moisture content of rayon cords. It is noticeable, therefore, that the moisture content is higher at elevated temperature and at high relative humidity conditions.

The objective of the thesis is to develop a test method in which rayon cords are dynamically tested with fixed moisture content at different temperatures. The developed $MCxTxRH$ diagram is extremely useful to Continental and to make it more acessible, a new way to display and visualize the data was proposed.

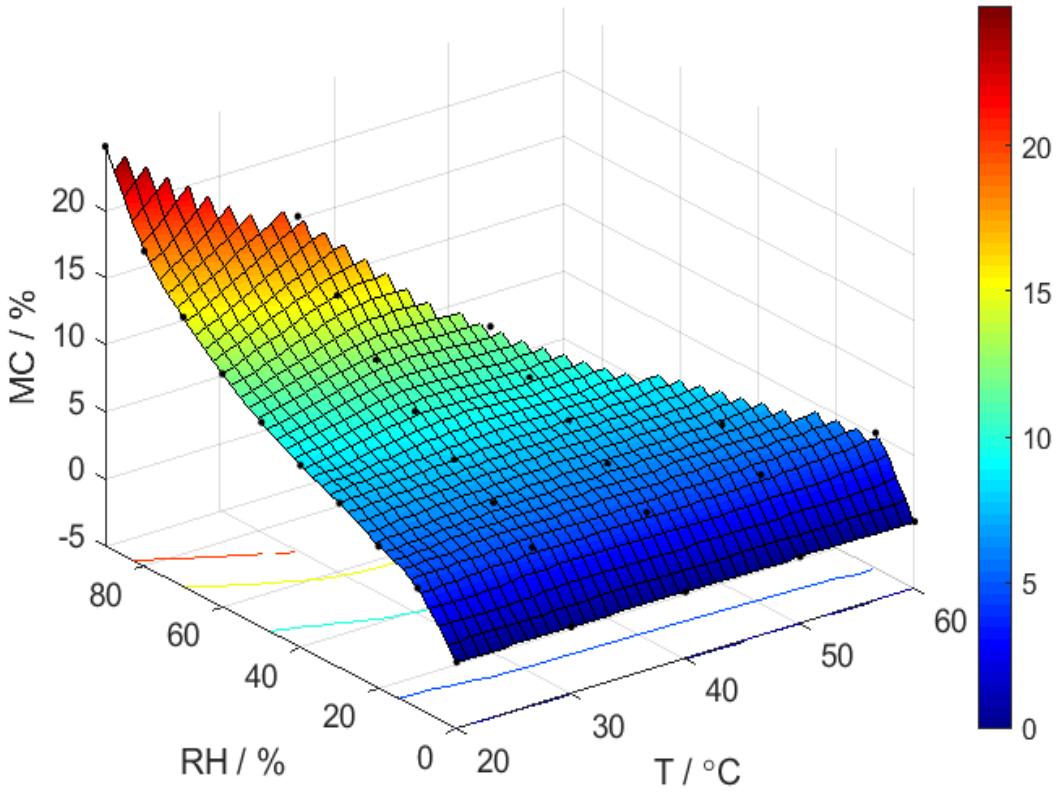

Figure 37: The new $MCxTxRH$ diagram developed for rayon cords.

That is, plotting the moisture content contour lines of the $MCxTxRH$ diagram. That idea was inspired by the weather forecast and topographic maps; the plot is illustrated in Figure 38. Each moisture content contour line of the $MCxTxRH$ diagram was named as one **"iso-moisture"** line.

An **"iso-moisture"** is therefore defined as a line which connects points of equal moisture content, at different atmospheric conditions of temperature and relative humidity. By following one "iso-moisture" line, one can easily and quickly choose the atmospheric conditions to be set up during the test, which will lead to a constant moisture content of textile. Consequently, the use of the "iso-moisture" tool, excludes the influence of the change in MC on the testing results, leading to a substatial improvement on the test reliability.

Both the $MCxTxRH$ and "iso-moisture" diagrams are new tools developed throughout this master thesis and they were presented for the first time at Continental. Their importance overcomes the testing method challenge mentioned above. That is because those diagrams have proven the extreme relevance of moisture control within rayon cords and they may be relevant for different departments at the company, such as: Test Method Development, Material Simulation, Material Process Development and Industrialization, Product and Supply Quality Control and Manufacturing.

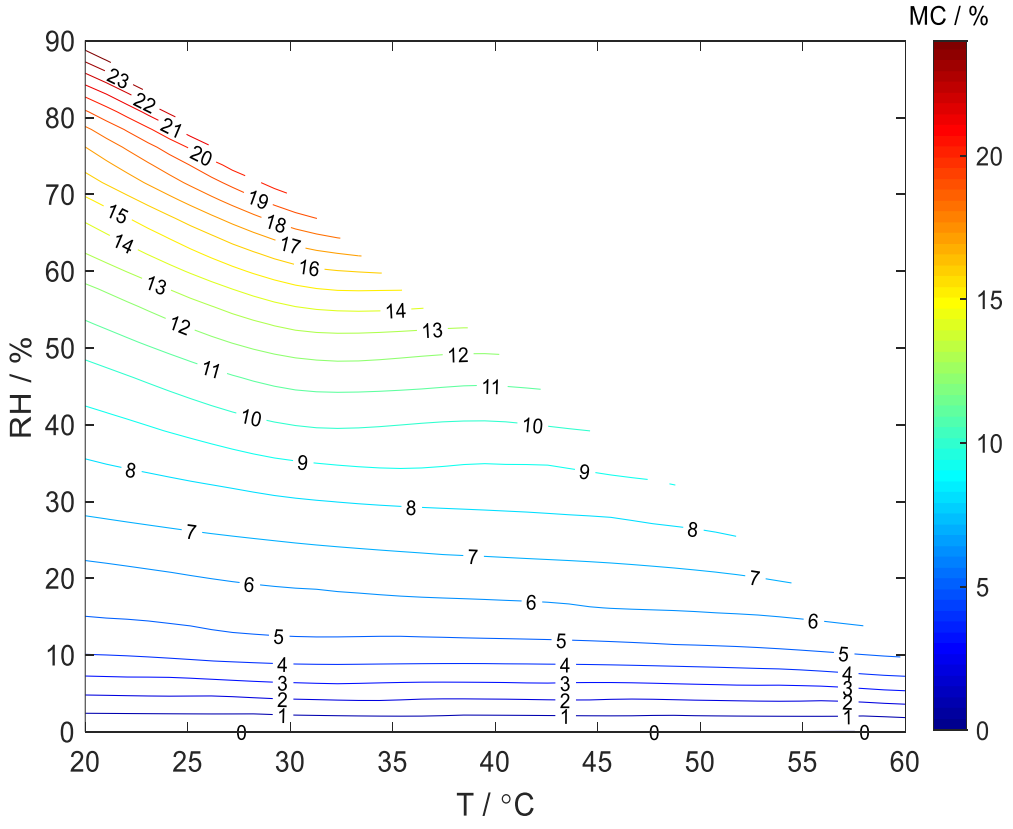

Figure 38: Diagram containing "iso-moistures" (%) for rayon cords.

4.4 Static and dynamic response of rayon cords under controlled conditions

4.4.1 Validation of the "iso-moisture" diagram

The iso-moisture diagram displayed in Figure 38 shows the pairs of temperature and relative humidity to be chosen in order to obtain the same moisture content within rayon after saturation. Each curve represents one iso-moisture, therefore, one saturation moisture content. To validate this diagram, two iso-moistures were chosen: the iso-moisture corresponding to MC = 8 % and the other to MC = 12.5 %.

Different atmospheres were set at the chamber connected to the MTS machine in order to have the same moisture content within the rayon. The detailed procedure was described in section 3.4.1 and the specifications presented in Table 7.

The Figure 39 shows the force-strain curve with a hysteresis loop for rayon 1840x2 at two different controlled atmospheres that led to a moisture content equal to 12.5 %. The curves are overlapping, which means the moisture content is indeed the same. Because of that, the iso-moisture diagram is validated for higher values of relative humidity.

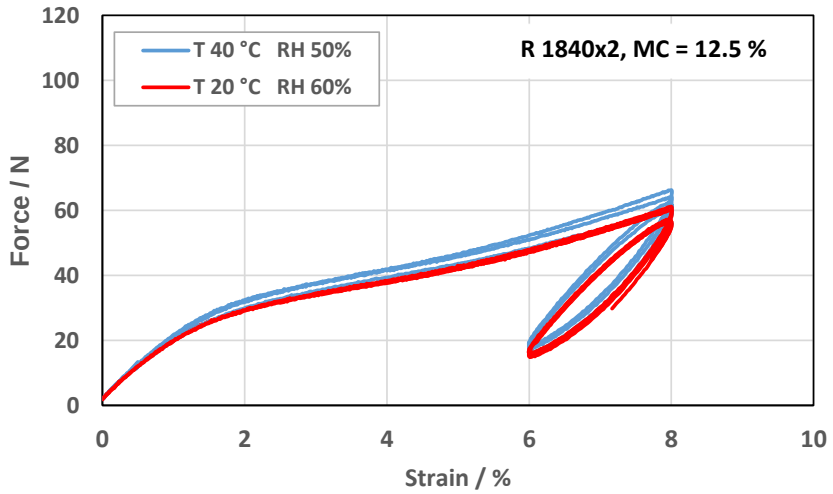

Figure 39: Force-strain curve with first hysteresis loop of rayon 1840x2, at MC = 12.5 %:

The test was also performed under different atmospheres that should result in moisture content equal to 8 %, as described in Table 7, and the results are showed in Figure 40. The curves also overlap; therefore, the iso-moisture diagram was validated for the lower range of relative humidity as well.

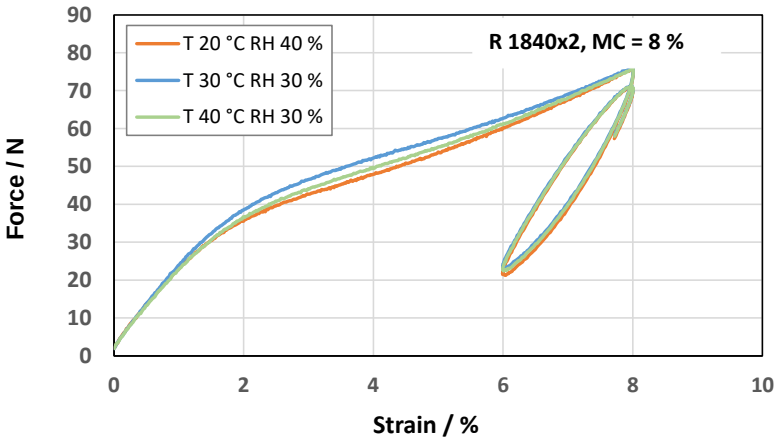

Figure 40 : Force-strain curve with first hysteresis loop of rayon 1840x2, at MC = 8 %.

The iso-moisture diagram was developed with data from rayon 1840x2. To validate the diagram for different constructions of rayon, the hysteresis elongation of rayon 2440x2 was also evaluated, following the iso-moisture 8 %. The force elongation curves for the two set up atmospheres for that fixed MC are presented in Figure 41. The curves also overlap, proving that the iso-moisture diagram can be utilized to predict moisture content of rayon cords 1840x2 and 2440x2.

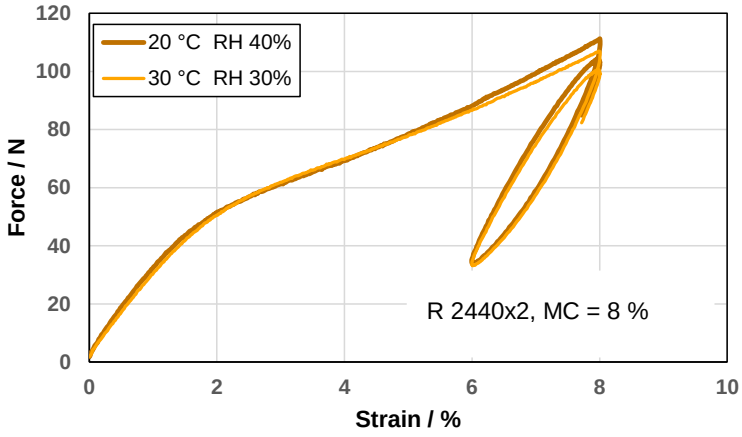

Figure 41:Force-strain curve with first hysteresis loop of rayon 2440x2, at MC = 8 %.

4.4.2 Dynamic mechanical analysis

The dynamic mechanical analysis was performed at different temperatures and frequencies to characterize rayon 1840x2. The relative humidity had to be controlled in a way that keeps the moisture content constant, excluding the effect of this variable on the DMA results.

The iso-moisture curves presented in Figure 38 were used to set up the atmospheric specifications for the DMA. The test was performed therefore at RH = 10 % because that is the lower limit of the chamber connected to the MTS machine, and that still guarantees a moisture content approximately constant. The temperatures 25 ˚C, 40 ˚C, 55 ˚C, 70 ˚C and 85 ˚C were tested at frequencies 20, 5, 2, 1, 0.2 and 0.1 Hz.

The elastic modulus (E') over frequency at different temperatures was derived from the results, and it is presented in Figure 42. The elastic modulus increases with the rise of frequency whereas the opposite is perceived with the grow of temperature, according to Figure 42.

The other parameters described in section 2.4.3, such as E'' and tan δ, which also give information about the viscoelastic characterization of the material, were obtained and presented in Appendix A.

A more in-depth analysis of the data to check the reliability of the test was done. For that, the raw signals obtained from the test were observed, that is the measured strain and stress signals. One example of hysteresis loop plotted from experimental values at 20 Hz is observed on the blue curve in Figure 43. This curve does not show a perfect ellipse shape because the stress and strain signal are not ideally harmonic. Because of that, an evaluation using Fast Fourier Transform (FFT) was done and the result is plotted on the red curve of Figure 43. The parameters were calculated from the red hysteresis loop, which are not overlapping the experimental data from blue curve. For the mismatched curves, the evaluation has no physical meaning. This is observed for temperatures 55 ˚C, 70 ˚C and 85 ˚C, after the 15th cycle, when the cord started to buckle.

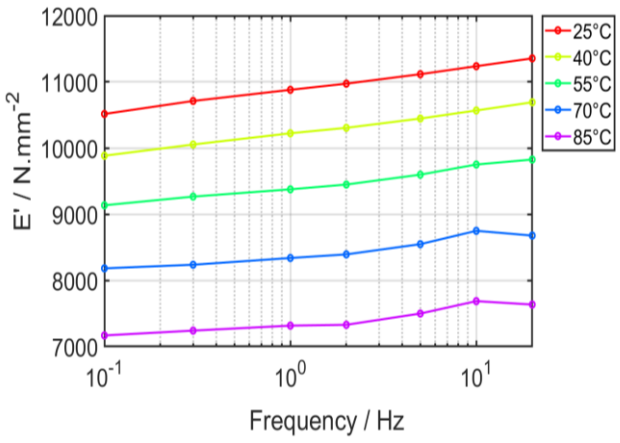

Figure 42: Elastic modulus of rayon 1840x2 over frequency, at different temperatures.

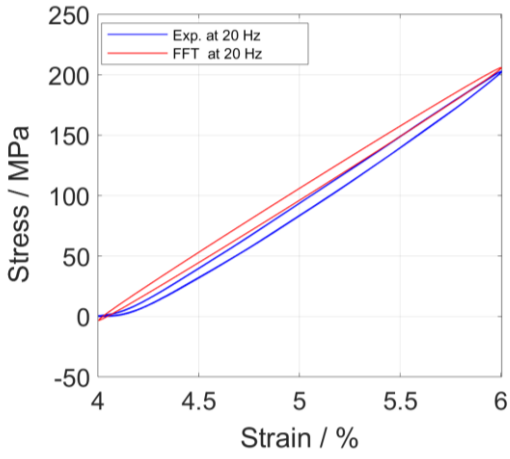

Figure 43: Example of hysteresis loop from raw test data and from FFT evaluation.

From the results above, it is conclusive that the conditions tested were not suitable for rayon cords. The test method must be improved in the future and it is suggested to choose a lower amplitude to avoid the cords buckling. On the other hand, the moisture content control worked, showing that the iso-moisture diagram can successfully be used to pick up atmospheric conditions to be set up in the chamber during the dynamic analysis. In conclusion, a reliable test method for rayon cords was created, which enables one to measure rayon cords dynamically with constant moisture content at different temperatures.

5 Conclusion

This master thesis provides new information regarding the effect of moisture on the mechanical response of rayon cords. Moreover, a reliable methodology was developed to keep the moisture content constant during the material characterization at different temperatures. In total, four distinct investigations regarding rayon material were successfully realized, and the achievements are described hereafter.

In the first one, it was proven that the water diffuses through the cured and uncured rubber used in tires and can reach the rayon cords within it. The force-strain curves of rubberized rayon cords showed that the presence of water vapor molecules decreases the stiffness of rayon cords. Dry cords presented a force of approximately 120 N while saturated cords 60 N, both at 8 % of strain. The skim compound delays the moisture uptake in comparison to bare cords; the effect of moisture on the mechanical properties is observed after a few days for uncured rubberized cords and after few weeks for cured cords. The second study proved that the mechanical properties are recovered after successive cycles of adsorption and desorption of water vapor molecules. Hysteresis elongation tests of rayon 1840x2 were carried out in the Zwick/Roel machine in order to perform the two studies described above.

The third investigation consisted of collecting data from TGA to draw the sorption isotherms of rayon cords at temperatures 20 ˚C, 30 ˚C, 40 ˚C, 50 ˚C and 60 ˚C. The isotherms were later represented in 3D plot diagram named $MCxTxRH$, which can be used to predict the moisture content (MC) within the saturated rayon cord at one given atmosphere (T and RH). The moisture content contour lines of the $MCxTxRH$ diagram was plotted, resulting in a 2D graph, where T is represented on the x-axis and RH on the y-axis. A new word - **“iso-moisture”** - was created to name each curve. One “iso-moisture” represents all the atmospheric conditions that lead to a constant saturation moisture content of rayon cords.

Finally, in the last and fourth part of the thesis, the new “iso-moisture” concept was validated for both cord constructions: rayon 1840x2 and rayon 2440x2. The cords went through static tests at MTS, which was configured for different atmospheric conditions, chosen following the same “iso-moisture” line. The tensile strength of the cords at different atmospheres was the same showing a constant moisture content. Furthermore, the first trial of dynamic mechanical analysis was carried out at MTS, with controlled RH = 10 %, chosen based on the “iso-moisture” tool. There were some limitations during the test regarding the applied strain and amplitude, which should be improved in future works.

Overall, the accomplishment of this dissertation has a great impact within Continental. The R&D Reinforcement department has approved the “iso-moisture” idea, which can later be used at different units within the company, which work with rayon 1840x2 and rayon 2440x2. For instance, for the creation of new test procedures regarding rayon cords, to improve the quality control of moisture content between suppliers and the plant and to predict tire performance in different countries or atmospheres.

6 Assessment of the Work Done

6.1 Objectives Achieved, limitation and future work

The main goal of the dissertation was achieved: the creation of a methodology to keep moisture content of rayon cords constant at different temperatures. Besides that, more in-depth information regarding rayon and its interaction with vapor molecules was provided. In other words, information about how the temperature and relative humidity of the air influences the adsorption of water molecules by rayon cords and how moisture content affects the tensile strength of the cords. Furthermore, how effectively a skim compound blocks the water diffusion and the recovery of the mechanical properties of rayon cords after successive cycles of adsorption and desorption of vapor molecules are also presented.

The main limitation of this project was the duration; the time was enough to perform only the first DMA trial for rayon 1840x2. Therefore, the “iso-moisture” curves should be later used to set the atmospheric conditions during the characterization of rayon 1840x2 and rayon 2440x2, at different states of amplitude, strain and temperature. The procedure itself must be optimized to find the suitable working range conditions for rayon, as previously done for nylon and polyester. The impossibility to measure moisture content during the tests was another limitation; therefore, the attachment of a balance to the MTS machine is recommended.

The learnings from this master dissertation also enables one to realize further scientific studies regarding rayon material. One suggestion is to investigate the kinetics of molecules water adsorption by rayon cords, that would be relevant to predict how long time the cords should be exposed to one particular atmosphere to obtain the desired moisture content. That information would be applicable for the manufacturing process and the quality supply control because rayon is exposed to different atmospheres in the different countries Continental is present.

6.2 Final assessment

I am glad for the opportunity to write my master dissertation at Continental headquarters. The overall experience was great, the team was supportive and helpful, and I enjoyed working with different cultures. During the project, I could combine the extensive knowledge learned from different courses at the university to solve practical challenges. I always felt my technical opinion was respected in the discussions, and that continuously motivated me. Moreover, I learned how the daily routine of a huge company is and could understand better how the R&D department works and its primary functions. After this experience, I do see myself following a career in R&D and would be happy to contribute again to Continental in the future.

7 References

[1] Aldhufairi, H. S., Olatunbosun, O. A. *"Developments in tyre design for lower rolling resistance: a state of the art review"*, Proceedings of the Institution of Mechanical Engineers, Part D: Journal of Automobile Engineering, 2017.

[2] Continental AG, *"Continental Divisions"*. Retrieved from (https://www.continental.com/en).

[3] Lindemuth, B.E., *"An Overview of Tire Technology",* The Pneumatic Tire, 2006.

[4] Kramer, T. *"Basic of Reinforcements"*, Continental tire academy, 2019.

[5] Continental Reifen Deutschland GmbH, *"Tyre Basics - Passenger Car Tyres",* 2013, available at https://blobs.continentaltires.com/www8/servlet/blob/85818/d2e4d4663a7c79ca81011ab47715e911/download-tire-basics-data.pdf?dl=t (Accessed September 2019).

[6] J. Chen, *"Synthetic Textile Fibers: Regenerated Cellulose Fibers"*, Textiles and Fashion, 2015.

[7] Woodings, C., *"A brief history of regenerated cellulosic fibers"*, Regenerated Cellulose Fibers, 2001.

[8] U.S. Code of Federal Regulations, *"Rules and regulations under the Textile Fiber Products Identification"*, Commercial Practices, 2001.

[9] Eichhorn, S.J., Hearle, J.W.S., Jaffe, M. and Kikutani, T., *"The structure of man-made cellulosic fibers"*, Handbook of textile fibre structure – Volume 2: Natural, regenerated, inorganic and specialist fibres, 2009.

[10] Lee, K.Y., Bismarck, A., *"Assessing the moisture uptake behavior of natural fibres"*, Interface engineering of natural fibre composites for maximum performance, 2011.

[11] Brunauer, S., "*Physical adsorption*", The adsorption of gases and vapors, Princeton University, 1943.

[12] Universitet Marie Curie, *"Adsorption at the solid/gas interface"*, Lublin.

[13] Keller, J., Reiner, S., "*Basic Concepts"*, Gas adsorption equilibria – Experimental Methods and Adsorption Isotherm, 2005.

[14] Zhang,H., "*The Permeability Characteristic of Silicone Rubber",* 2006.

[15] Zeid, A., Othman, A. L., "*A Review: Fundamental Aspects of Silicate Mesoporous Materials",* 2012.

[16] Sousa, L.H., Pereira, N., Lima, O., and Fonseca, E., *"Equilibrium moisture isotherms of textile materials.",* Universidade Estadual de Maringá, 2001.

[17] Barbosa, D., *"Secagem e Humidificação"*, Apontamentos de Processos de Separação I, 2016.

[18] Ashour, T., Georg, H., Wu, W., "*An experimental investigation on equilibrium moisture content of earth plaster with reinforcement fibres for straw bale buildings"*, Applied Thermal Engineering, 2010.

[19] Vaisala, Humidity Conversion Formulas, 2013, available at https://www.hatchability.com/Vaisala.pdf (Accessed in December 2019).

[20] METTLER TOLEDO, *"Thermal Analysis Information for Users - User Com 24"*, 2006, available at https://www.mt.com/us/en/home/ (Accessed in November 2019).

[21] Wootton, D.B*., "Production and Properties of Textile Yarns",* The Application of Textiles in Rubber, 2001.

[22] Wagner W., Pruß A., *"The IAPWS Formulation 1995 for the Thermodynamic Properties of Ordinary Water Substance for General and Scientific Use",* Journal of Physical and Chemical Reference Data, 2002.

[23] Gomes, M., *"Hysteresis in Tyre Textile Reinforcements*", 2018.

[24] Rosato, D.V., *"Design Parameters",* Plastics Engineered Product Design, 2003.

[25] Samui, B. K., Prakasan, M. P., Chakrabarty, D. and Mukhopadhyay, R. *"Hysteresis characteristics of high modulus low shrinkage polyester tire yarn and cord",* Rubber Chemistry and Technology, 2011.

[26] Callister, W.D., *"Characterization, Applications, and Processing of Polymers"*, Materials Science and Engineering, 2009.

[27] Barsoum, R.G., *"Modification and Engineering of HSREP to Achieve Unique Properties",* Elastomeric Polymers with High Rate Sensitivity, 2015.

[28] Ebnesajjad, S., *" Surface and Material Characterization Techniques"*, Surface Treatment of Materials for Adhesion Bonding, 2006.

[29] PERKIN ELMER, *"Thermogravimetric Analysis (TGA)"*, A begginer's Guide, 2015.

[30] Ph.D. Hongying Zhao. H., TU Clausthal – Institut für Polymerwerkstoffe und Kunststofftechnik (to be published in 2020).

[31] Engelund, E.T., Thygesen, L.G., Svensson, S. and Hill, C.A.S., *"A critical discussion of the physics of wood-water interactions"*, 2012.

Annex A - Impact of moisture adsorption on mechanical properties of rayon cords

There was one internal study at Continental done by Christian Neufeld in which dry sample of rayon cords were exposed to the laboratory conditions (T = 23 °C and RH = 55 %) different time duration (0, 10, 20, 30, 50, 60, 120 min). Later the force elongation was evaluated, as well as the total mass of the cord before being tested. The results are illustrated in Figure 44. There is a significant drop in the tensile strength along with the raise of moisture content, which increases with exposure time. From this study, it was also observed that the moisture content reaches a value close to the saturation condition, after two hours of exposure to the surrounding atmosphere.

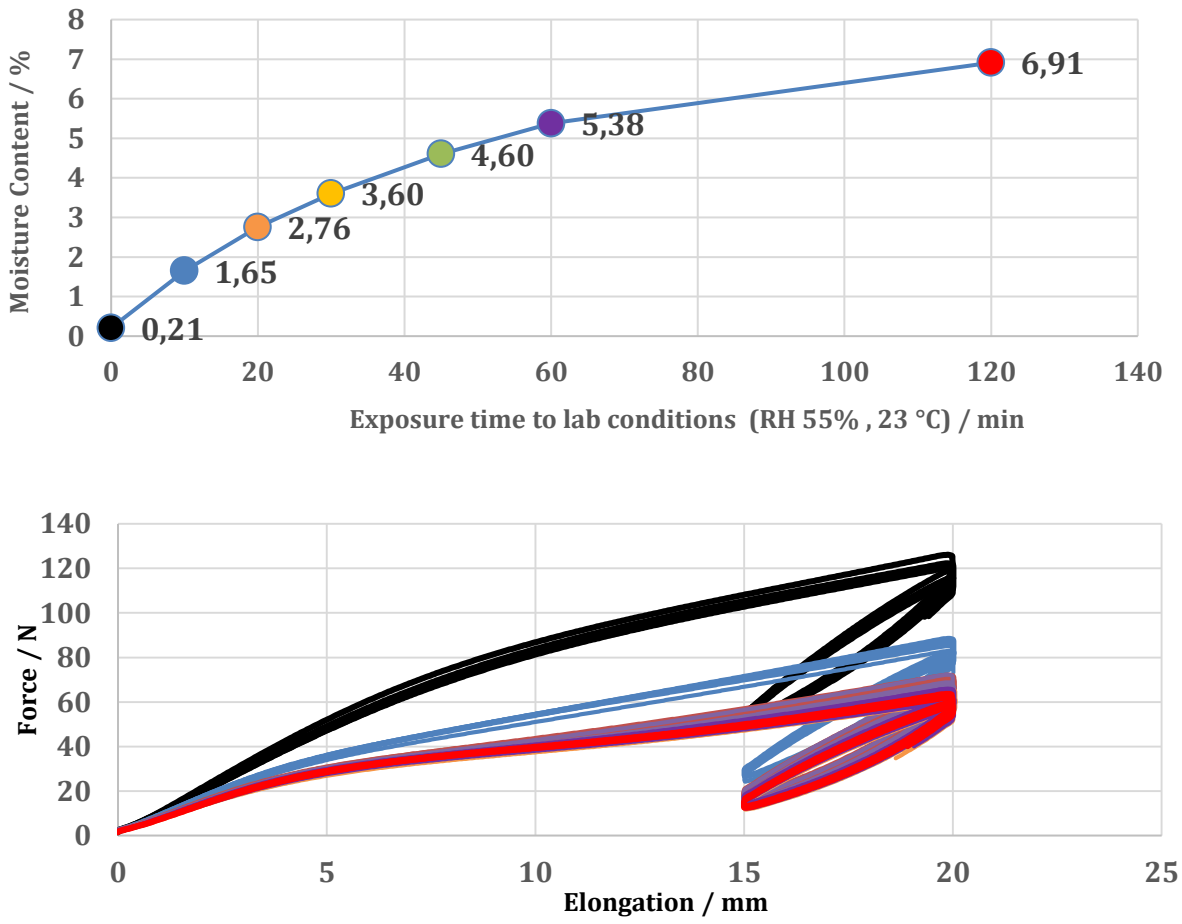

Figure 44: The moisture content of rayon cords over time (above) and the respective force elongation curve with hysteresis loop (below).

Annex B – TGA working range

The figure below shows the working range of the TGA/DSC 2 from METTLER TOLEDO to be used in order to avoid the dew point and, therefore, prevent the damage of the machine.

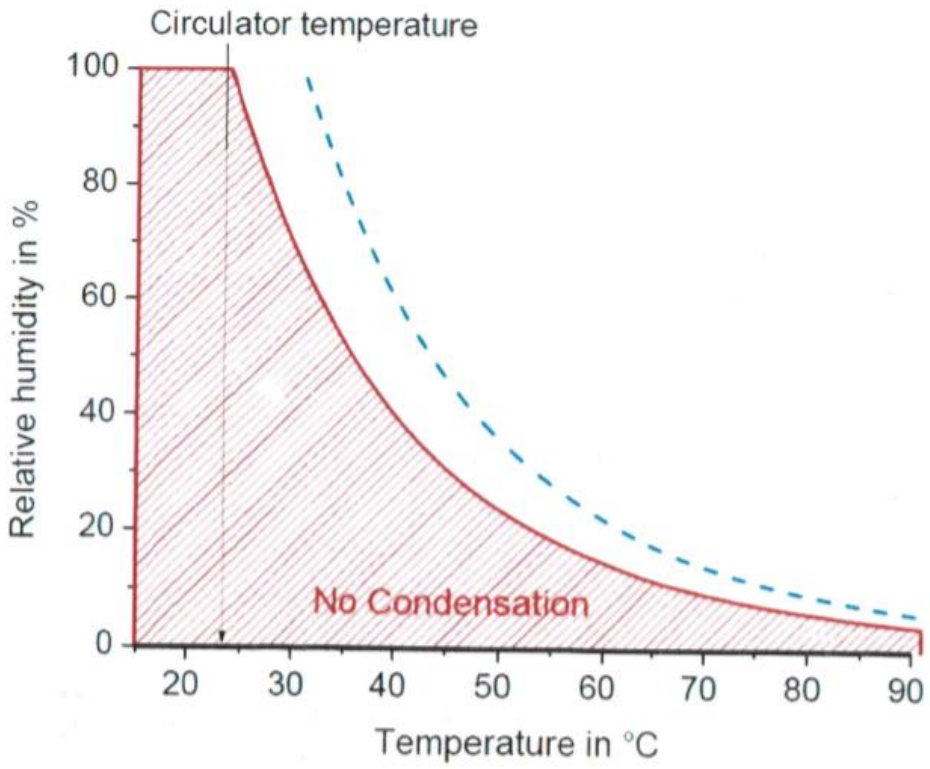

Figure 45: Working conditions at TGA/DSC 2 to avoid dew point.

Appendix A - DMA results for Rayon

The elastic modulus and the damping coefficient obtained at the first DMA trial of rayon cords, which were perfumed according to the test method described in section 3.4.1, are presented in the figures below:

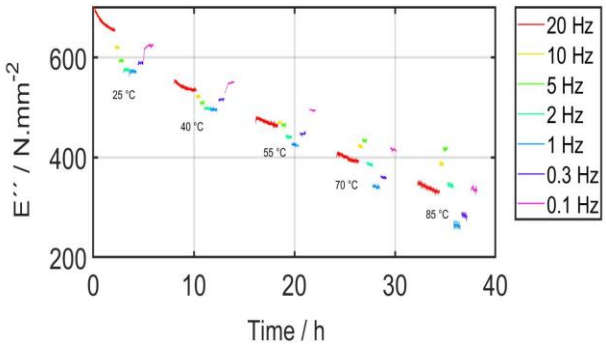

Figure 46: Viscous modulus of rayon 1840x2 over time at different temperatures.

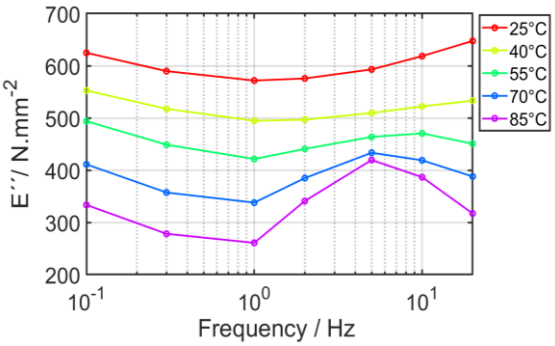

Figure 47: Viscous modulus of rayon 1840x2 over frequency at different temperatures.

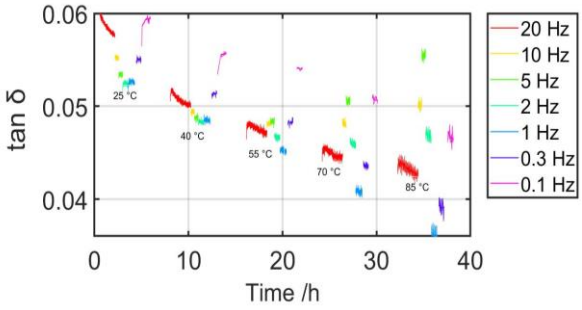

Figure 48: Damping coefficient of rayon 1840x2 over time, at different temperatures.

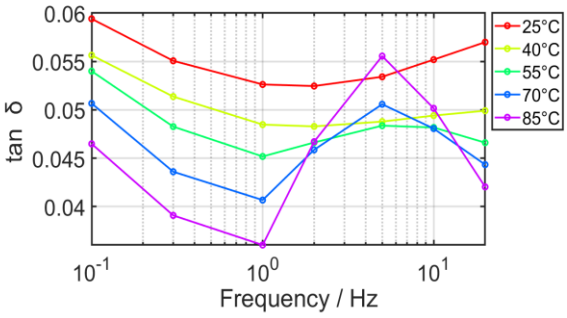

Figure 49: Damping coefficient of rayon 1840x2 over frequency, at different temperatures.